

Development of an aptamer based optical Nano-biosensor for on-site diagnosis of Vibriosis in Aquaculture

A Dissertation for

Course code and course title: MBT 651- Dissertation

Credits: 16

Submitted in partial fulfilment of Master's Degree

M.Sc. in Marine Biotechnology

by

MARIYA HUSSAIN

22P0500010

ABC ID: 219386878854

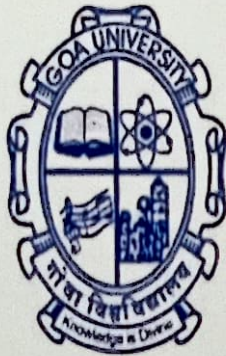
202207104

Under the supervision of

Dr. SAMANTHA FERNANDES D'MELLO

School of Biological Sciences and Biotechnology

Biotechnology Discipline



GOA UNIVERSITY

Date: 8th April 2024



Seal of the school

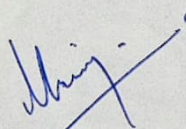
Examined by:

Sanita
8/4/24
Phonkar
08/4/2024
Sanitahachau
8/4/24
Dr. P. P. ...
Dr. ...
8/4/24

DECLARATION BY STUDENT

I hereby declare that the data presented in this Dissertation report entitled, “**Development of an aptamer based optical Nano-biosensor for on-site diagnosis of Vibriosis in Aquaculture**” is based on the results of investigations carried out by me in the School of Biological Sciences and Biotechnology, Goa University under the Supervision of Dr. Samantha Fernandes D’Mello and the same has not been submitted elsewhere for the award of a degree or diploma by me. Further, I understand that Goa University or its authorities will not be responsible for the correctness of observations / experimental or other findings given the dissertation.

I hereby authorize the University authorities to upload this dissertation on the dissertation repository or anywhere else as the UGC regulations demand and make it available to any one as needed.



Ms. Mariya Hussain

22P0500010

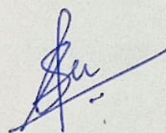
Marine Biotechnology

Date: 8th April 2024

Place: Goa University

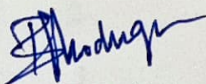
COMPLETION CERTIFICATE

This is to certify that the work entitled, "**Development of an aptamer based optical Nanobiosensor for on-site diagnosis of Vibriosis in Aquaculture**" is a bonafide work carried out by Ms. Mariya Hussain under my supervision at the School of Biological Sciences and Biotechnology, Goa University in partial fulfilment of the requirements for the award of the degree of Master of Science in Marine Biotechnology at the School of Biological Sciences and Biotechnology, Goa University.



Dr. Samantha Fernandes D'Mello

Marine Biotechnology



Prof. Bernard F. Rodrigues

Sr. Professor and Dean

School of Biological Sciences and Biotechnology

Date: 8/14/24

Place: Goa University

Dean of School of Biological Sciences
& Biotechnology
Goa University, Goa-403206

CONTENTS

Chapter	Particulars	Page numbers
	Preface	v
	Acknowledgments	vi
	Tables and Figures	viii-ix
	Abbreviations	x
	Abstract	xi
1.	Introduction	1-7
	1.1 Background	
	1.2 Aim and objectives	
	1.3 Hypotheses	
	1.4 Scope	
2.	Literature Review	8-16
3.	Methodology	17-24
4.	Analysis	25-39
	Future prospects and	40
	Conclusion	
	References	41-50

PREFACE

Aquaculture or farming of aquatic organisms plays a pivotal role in meeting the growing global demand for seafood and contributes significantly to food security and economic growth worldwide. However, the industry faces major challenges, particularly concerning the health and management of aquatic organisms. Among the various threats encountered, the presence of bacterial pathogens poses a significant concern, particularly *Vibrio* species, which can cause devastating diseases in aquaculture species.

In the pursuit of effective disease management strategies, the development of rapid and accurate diagnostic tools is imperative. This dissertation explores the application of aptamer-based nano-biosensors for the rapid diagnosis of vibriosis, a prevalent disease caused by *Vibrio* species, in aquaculture settings. Aptamers, single-stranded DNA or RNA molecules selected to bind specifically to target molecules, offer numerous advantages as recognition elements in biosensors, including high specificity, sensitivity, and versatility.

The primary objective of this research is to design, develop, and evaluate an aptamer-based nano-biosensor capable of detecting *Vibrio* pathogens accurately in aquaculture environments. Through a combination of molecular biology techniques, nanotechnology, and biosensor development methodologies, this dissertation aims to help improve the tools used to diagnose problems in aquaculture.

ACKNOWLEDGEMENT

I offer my sincere thanks to God for granting me the strength and perseverance to overcome obstacles and achieve my academic goals.

I would like to express my heartfelt gratitude to the Department of Biotechnology (DBT) for sponsorship throughout the duration of my dissertation work. Their financial assistance played a pivotal role in the successful completion of this research endeavor.

I extend my deepest appreciation to the Dean of the School of Biological Sciences Biotechnology, Prof. Bernard F. Rodrigues, to the Vice-Deans, to the Program Director of Marine Biotechnology, Prof. Sanjeev Ghadi and to all the esteemed faculty members of the Department of Biotechnology whose guidance, encouragement, and invaluable insights have been instrumental in shaping my academic journey.

Special thanks to my guide, Dr. Samantha Fernandes D'Mello, whose mentorship, wisdom, and unwavering support have been crucial in steering me through the challenges of research. Your encouragement, constructive feedback, and guidance have been invaluable assets, and I am profoundly grateful for your mentorship.

I am immensely grateful to Dr. Pranay Morajkar and his dissertation student Prateek, from the School of Chemical Sciences, Goa University for being a constant help throughout my project work.

I am thankful to all the non-teaching staff Sandhaya ma'am, Serrao sir, Sameer sir, Ashish sir, Sanjana ma'am, Popkar sir and Jaya ma'am for facilitating the experimental aspects of this

study. I would like to acknowledge the PhD scholars, especially Hetika and Priti ma'am whose shared experiences have helped me a lot.

I would like to thank Prajot Chari sir, Chemistry Discipline, Goa University for helping with the FTIR analysis, Sophisticated analytical Instrumentation Facility (SAIF), IIT Bombay for TEM imaging and Central Sophisticated Instrumentation Facility, BITS, Goa for the zeta potential measurement.

I extend my deepest gratitude to my beloved family for their unconditional love, encouragement and support in completing my dissertation work.

Lastly, my sincere thanks to all my friends, especially Manasi Rane, MalavikaVino and Aarushi Doshi for their constant help and support.

TABLES

Table no.	Description	Page no.
Table 1	Recent biosensors for <i>Vibrio</i> sp. detection	11
Table 2	Aptamer-based biosensors reported for different pathogen with colorimetric detection.	16
Table 3	Optical density measured for different volumes of bacterial samples at different growth stages.	37
Table 4	Absorbance at 490 nm.	39

FIGURES

Figure no.	Description	Page no.
Figure 1	Reflux condenser apparatus with gold solution (yellow)	18
Figure 2	Optical image of Apt-MNPs	21
Figure 3	Isolated colonies from fish and shrimp sample on TCBS agar plates	24
Figure 4	Red colloidal solution of AuNPs	25
Figure 5	UV-Visible absorption spectra of AuNPs (Peak at 522 nm)	26
Figure 6	SEM image of AuNPs	26
Figure 7	TEM image of AuNPs	26
Figure 8	FTIR analysis of the AuNPs	27
Figure 9	Zeta potential analysis of the AuNPs	28
Figure 10	Optical images of (A) AuNPs, (B) Apt-AuNPs+ NaCl, (C) AuNPs+ NaCl respectively	29
Figure 11	UV- Visible absorption spectra of Apt-AuNPs (Peak at 526 nm)	30
Figure 12	UV-Visible absorption spectra of AuNPs+ NaCl	30
Figure 13	FTIR image of Apt-AuNPs conjugate	31
Figure 14	Test for magnetic property	32
Figure 15	SEM image of MNPs	32
Figure 16	XRD pattern of MNPs	33
Figure 17	FTIR spectra of ascorbic acid	34
Figure 18	FTIR spectra of carboxyl functionalized MNPs	34
Figure 19	Zeta potential of MNPs	35
Figure 20	Zeta potential of Apt-MNPs	35
Figure 21	Growth curve of <i>V. alginolyticus</i>	36
Figure 22	Optical images of the colorimetric detection (A) Apt-AuNPs+ MNPs+ buffer (B) Apt-AuNPs+ MNPs+ bacteria + buffer	38
Figure 23	Raw fish and shrimp sample from local market	39

ABBREVIATIONS

Abbreviation	Entity
°C	Degree Celsius
μg	Microgram
μL	Microliter
mL	Milliliter
M	Molar
mM	Millimolar
nm	Nanometer
NPs	Nanoparticles
AuNPs	Gold nanoparticles
MNPs	Magnetic nanoparticles
Apt	Aptamer
Apt- AuNPs	Aptamer- gold nanoparticles conjugate
Apt- MNPs	Aptamer- magnetic nanoparticles conjugate
AA	Ascorbic acid

ABSTRACT

This study aimed to develop a rapid, and sensitive screening method to effectively prevent and control the spread of fish disease, particularly caused by *Vibrio alginolyticus*. The approach involved the creation of a simple visual colorimetric assay utilizing MNPs and AuNPs for the detection of *V. alginolyticus*. Initially, we conjugated an aptamer specific to *V. alginolyticus* onto the surface of MNPs, which served as a specialized magnetic separator. Simultaneously, another aptamer was immobilized on the surface of AuNPs, functioning as a colorimetric detector. Upon encountering *V. alginolyticus*, a sandwich structure consisting of MNP–aptamer–bacteria–aptamer–AuNPs was formed through the specific recognition between the aptamer and *V. alginolyticus*. Utilizing the magnetic separation technique, we generated a detection signal. Leveraging the optical properties of AuNPs, a visual signal was observed, enabling instrument-free colorimetric detection. Furthermore, we applied this method to detect *V. alginolyticus* in locally bought raw shrimp and fish samples. This preliminary study underscores the potential of our developed assay as an efficient tool, offering promising prospects to design a strip-based biosensor for rapid detection of *V. alginolyticus*.

CHAPTER 1: INTRODUCTION

1.1 Background

Aquaculture and fisheries stand as one of the fastest-growing industries, reaching a global production of 85.3 million tons in 2019. (Tacon et al., 2020). Production surged significantly, surpassing a threefold increase in live-weight volume from 34 million metric tons (Mt) in 1997 to 112 Mt in 2017. Seaweeds, carps, bivalves, tilapia, and catfish were the key contributors to most of the aquaculture output in 2017. Freshwater fish comprise 75% of the global edible aquaculture volume (Edward et al., 2019). In 2017, Asia retained its position as the leading aquaculture producer, responsible for 92% of the live-weight volume of animals and seaweeds (FAO 2019). Countries renowned for aquaculture species diversity are situated in Asia, with China notably leading by a considerable margin. (Metian et al., 2020). India currently holds second position, with a coastline spanning 7,517 km with an extensive network of rivers and canals totaling approximately 195,210 km, which includes 14 major rivers, 44 medium rivers, and numerous small rivers and streams (De Jong et al., 2017), presenting enormous potential for the development of aquaculture (FAO 2014).

However, modern aquaculture systems encounter numerous challenges, especially in water quality management, disease control, feed development, hatchery and grow-out technologies (Jena et al., 2017). The high densities of fish rearing employed in aquaculture facilitate the transfer and spread of pathogenic microorganisms, often serving as a primary cause of catastrophic outbreaks (Rohani et al., 2022). With such intensive farming systems, the rise in infectious diseases has negatively affected the expansion of marine fish farming worldwide as waterborne pathogens have the capacity to spread at accelerated rates compared to terrestrial

systems (McCallum et al., 2003). Indeed, infectious disease stands as the leading cause of mortality among farmed fishes (Pillay & Kutty, 2005). An outbreak can frequently result in the complete loss of fish stocks, necessitating expensive decontamination of facilities and equipment. This issue has been recognized as a potential constraint to aquaculture production (Jansen et al., 2012).

In China, India, and Vietnam, fish diseases are estimated to account for over 30% of the total production loss (Mohd-Aris et al., 2019). When a disease outbreak occurs, it can result in mass mortalities, economic losses to the farmers, and environmental impacts such as contamination of water bodies (Jørgensen et al., 2020). Some of the diseases arise from attacks by pathogenic bacteria, particularly Gram-negative bacteria, and to a lesser extent, Gram-positive bacteria (Maldonado-Miranda et al., 2022). The bacterial infections like *Aeromonas septicemia* (Thirumalaikumar et al., 2021), Edwardsiellosis (Buján et al., 2018), Columnaris (Declercq et al., 2013), Streptococcosis (Luo et al., 2017), and Vibriosis (Ji et al., 2020) have been reported in the aquaculture industry.

Vibriosis is a common bacterial disease affecting various marine fish and shellfish. According to Chong et al., (2011), about 66.7% of reported diseases in groupers (*Epinephelus spp.*) are due to vibriosis, leading to mortality rates of up to 50% (Liao et al., 2008; El-Gali-Mohamed et al., 2012). Different species of Vibrionaceae, including *Vibrio parahaemolyticus*, *V. alginolyticus*, *V. harveyi*, *V. owensii*, and *V. campbelli*, have been associated with health issues in farmed aquatic animals (Nor-Amalina et al., 2017). Typical indicators of *Vibrio*-related disease encompass lethargy, tissue and appendage decay, reduced growth and metamorphosis rates,

body deformities, bioluminescence, muscle cloudiness, and melanization (Aguirre-Guzman et al., 2004). Additionally, infected fish exhibit skin discoloration, red necrotic lesions in the abdominal muscle, and erythema (bloody patches) around the vent, base of fins, and within the mouth (Anderson and Conroy, 1970).

Vibrio species, naturally diverse in their environment, exchange genetic material, including toxigenic genes, through horizontal transfer. This process can transform non-toxigenic strains with epidemic potential. Thus, continuous surveillance of these *Vibrio* species' toxigenic and non-toxigenic strains is essential to prevent outbreaks (Azarian et al., 2016). Fast, accurate, and sensitive methods for identifying *Vibrio* infections early can ensure timely treatment. Moreover, easy-to-use detection techniques can be highly beneficial in regions where there is limited access to laboratories performing traditional bacterial culture methods.

Among all the species, *Vibrio alginolyticus* is considered an important opportunistic fish pathogen. Various outbreaks linked to *V. alginolyticus* have been reported in aquaculture farms. Infection with *V. alginolyticus* results in high mortality rates among aquaculture animals such as shrimp, shellfish, fish, and seahorses (Manchanayake et al., 2023). It is also a major cause of seafood-related bacterial gastroenteritis worldwide, commonly associated with consuming raw or undercooked seafood (Cai et al., 2007).

To monitor *V. alginolyticus*, different detection methods have been developed. The standard method involves using a specialized plate culture medium for detection which offers high accuracy, however, it's a lengthy and complicated process, not suitable for rapid detection needs (Yin et al., 2018). Various molecular biology techniques, including enzyme-linked

immunosorbent assay (ELISA), polymerase chain reaction (PCR), loop-mediated isothermal amplification (LAMP), recombinase polymerase amplification (RPA), and immunofluorescence assay (IFA) have been used to detect *V. alginolyticus* (Hui-Min et al., 2020). However, these methods often involve trained personnels, longer detection times and complex procedures. Additionally, the presence of challenging pollutants like aerosols can lead to non-specific amplification and false positives, reducing accuracy.

Immunology-based detection methods rely on antigen-antibody interactions but are costly and susceptible to unstable results due to the fragility of monoclonal antibodies (Hayrapetyan et al., 2023). Given the epidemiological importance of *Vibrio* species and their potential to cause outbreaks, timely identification of the causative agents is essential for initiating an effective response and treating the disease efficiently. Therefore, there's a need for new, more reliable detection methods for *V. alginolyticus*.

In recent decades, biosensing platforms, particularly biosensors, have emerged as appealing and efficient alternatives for detecting microorganisms in clinical diagnosis, food analysis, and environmental monitoring (Poltronieri et., 2014; Yoo et al., 2016). Biosensing strategies hold great promise as they save time, are cost-effective, practical, and capable of real-time analysis (Hushiarian et al., 2015; Tian et al., 2016). Biosensors typically comprise two essential elements: a bioreceptor, which detects the target analyte (such as an antibody, aptamer, or complementary DNA sequence), and a transducer, which converts the resulting biochemical reaction into a measurable signal.

Aptamers are single-stranded DNA or RNA that can fold into secondary and three-dimensional structure, enabling them to recognize various target molecules with high specificity and affinity. Aptamers have emerged as an increasingly important molecular tool for both diagnostics and therapeutics. Aptamers or chemical antibodies possess numerous advantages as recognition elements in biosensing. They are small, chemically stable, and cost-effective (Song et al., 2008). Additionally, aptamers offer remarkable flexibility and convenience in structure design, resulting in the development of novel biosensors with high sensitivity and selectivity. Recently, the integration of aptamers with innovative nanomaterials has notably enhanced the performance of aptamer-based sensors.

This study is centered on developing an aptamer-based biosensors using two distinct nanoparticles as substrates to specifically detect whole cell *V. alginolyticus*, potentially serving as a diagnostic method for Vibriosis. Aptamers targeting the pathogen's outer membrane act as the recognition element. Moreover, the characteristics of gold and magnetic nanoparticles have been explored for simple colorimetric signal detection.

1.2 Aim and Objectives

Aim: To design a simple optical aptamer-based nano biosensor for the rapid and easy detection of *Vibrio alginolyticus* in aquaculture farms.

Objectives:

1. To synthesize and characterize gold and magnetic nanoparticles.
2. To identify specific aptamers for *V. alginolyticus* and facilitate their binding to the synthesized nanoparticles.
3. To characterize the aptamer-nanoparticle (Apt-NP) conjugates.
4. To standardize the in-vitro detection of the pathogen by the Apt-NP conjugate.

1.3 Hypothesis

In this research, we utilize the sandwich formation concept, employing two different aptamers that bind to separate nanoparticles. Aptamer 1 will be attached to the surface of gold nanoparticles (AuNPs) and used as a colorimetric sensor. Additionally, Aptamer 2, which is designed to detect *V. alginolyticus*, will be linked to the surface of magnetic nanoparticles (MNPs) to function as a specific magnetic separator. The process of attaching aptamers to MNPs will be facilitated by a bond formation mechanism involving the carboxyl groups of COOH-functionalized MNPs and the amino groups of amino-modified aptamers. When encountering *V. alginolyticus*, a sandwich-like structure composed of AuNPs–aptamer 1–bacteria–aptamer 2–MNPs is formed due to the specific interaction between the aptamers and *V. alginolyticus*. Subsequently, magnetic separation will be employed to generate a detection signal.

1.4 Scope

The colorimetric assay can be utilized as a rapid and sensitive detection of *V. alginolyticus* in water and seafood products, such as shrimp, oysters, and fish, aiding in ensuring food safety and preventing disease outbreaks. The developed technology can be used in future diagnostic kits which could help the farmers with the onsite detection of vibriosis without the need for sophisticated lab and facilities.

It can be employed for monitoring *V. alginolyticus* contamination in water sources, particularly in coastal areas where aquaculture activities are prevalent and seafood products. This could help in assessing the risk of exposure and implementing appropriate mitigation measures.

CHAPTER 2: LITERATURE REVIEW

2.1 *Vibrio alginolyticus*

Vibrio alginolyticus, belonging to the *Corynebacterium* genus, is commonly found in marine, estuarine, and other aquatic environments globally. This zoonotic pathogen is a significant cause of economic losses in the aquaculture sector and ranks as the second most common cause of human *Vibrio* infections (Wang et al., 2021). It causes one of the major bacterial diseases, Vibriosis in fish and shrimp aquaculture (Ringø et al., 2020).

According to Chong et al. (2011), it affects all stages of growth, leading to mortality for up to 50%. The symptoms include hemorrhagic septicemia with extensive external skin lesions, necrosis of some organs and tissue, erosion of tail, pale kidney, dark pigmentation, exophthalmic eyes, (Kahla-Nakbi et al., 2007; Haldar et al., 2010). The literature on the impact of *Vibrio alginolyticus* on various fish species reveals a distribution of affected species across different regions. Among the species affected by this pathogen, In India, Cobia and Asian seabass (Rathore et al., 2013; Rameshkumar et al., 2014), *Penaeus monodon* (Selvin et al. 2003) have been reported. In China, Crimson snapper (Cai et al. 2013), Large yellow croaker (Chen et al. 2008), *Litopenaeus vannamei* (Liu et al., 2004) have been identified as susceptible to *Vibrio alginolyticus*. These findings highlight the diverse geographic distribution and host range of *Vibrio alginolyticus* infection in aquaculture farms. With the increasing incidence of vibriosis causing severe outbreaks in the aquaculture farms, attempts for early detection is a major concern to help the farmers in preventing economic loss.

2.2 Conventional methods for pathogen detection

Over the years, *V. alginolyticus* has been identified using traditional techniques of cultivating pathogens on various selective or differential media (Xuedong and Yuqing, 2015). While these traditional methods have been successful in diagnosing the pathogenic bacteria in food, water, and the environment, they are time-consuming, and take days to grow at a quantifiable concentration (Zeng et al., 2018). Additionally, these methods have limitations including low sensitivity, poor specificity, and require labor-intensive and time-consuming analysis.

Traditional techniques like bacterial culture methods utilized for meat, poultry and water samples, have an incubation time up to 48 hours (Buss et al., 2019; Gill, 2017; Bargellini et al., 2011) and the biochemical tests yield results for drinking water contamination in 24 hours (Hinić et al., 2017; Chauhan et al., 2017). ELISA detects contamination in drinking and aquatic water in under 3 hours (Zhang et al., 2016; Su et al., 2016), metagenomics offers insights into irrigation water contamination within 24 hours (Maguire et al., 2021), Nucleic Acid Sequence-Based Amplification (NASBA) detects tap water contamination in 12 hours (Zhai et al., 2019), Loop-Mediated Isothermal Amplification (LAMP) provides detection in milk, pork, beef, and marine water samples in 40 minutes to 1 hour (Mei et al., 2019; Lee et al., 2019) and PCR detection of samples takes around 16 hours (Ibekwe and Grieve, 2003).

Moreover, various methods developed to identify *V. alginolyticus* infection, including polymerase chain reaction (PCR), real-time PCR, immunofluorescence antibody testing, and loop-mediated isothermal amplification (LAMP), have been primarily used for pathogen detection in laboratory research rather than for definitive diagnosis by farmers in mariculture

farms due to several drawbacks such as complex procedures, costly reagents, lengthy processing times, and demanding environmental requirements. Hence, there is an urgent need for novel detection techniques to enable rapid diagnosis of *V. alginolyticus* infection in mariculture farms (Duan et al., 2016).

Despite the technical advancements of the analytical tools, the existing techniques for detecting the pathogen are often characterized by high costs, limited sensitivity, and lack of rapid detection capabilities. Therefore, advanced technologies like biosensors for rapid, precise, and sensitive pathogen identification play a crucial role in enabling early prevention of *Vibrio* infections and ensuring timely treatment (Loo et al., 2022).

2.3 Biosensors and their types

Biosensors function by detecting analytes in biological or chemical reactions and produce signals corresponding to the concentration of the analyte. Biosensors can be categorized based on the type of signal they generate, including electricity, heat, or light. A standard biosensor comprises components such as the analyte, bioreceptor, transducer, electronics, and display (Bhalla et al., 2016).

Compared to other bacteria detection techniques, biosensors offer characteristics including rapidity, specificity, sensitivity, and reliability. When fabricating biosensors, the primary concern is to create sensitive, and specific devices that remain unaffected by environmental factors such as temperature and pH (Mehrotra et al., 2016). Table 1 presents a summary of various types of biosensors developed for *Vibrio* species, employing diverse detection techniques such as electrochemical, Nuclear Magnetic Resonance (NMR), piezoelectric, colorimetric, and fluorescence.

Table 1. Recent biosensors for *Vibrio* sp. detection

Sr. no.	Pathogen	Description	Detection Technique	Reference
IMMUNOSENSORS				
1.	<i>V. Cholera</i>	A simple, efficient, and label-free biosensing platform based on nanostructured gadolinium oxide nanoparticles (Gd ₂ O ₃ NPs).	Electrochemical	Kumar et al., 2023
2.	<i>V. parahaemolyticus</i>	A 96-well plate coated with VP antibody captures the target VP, which then binds the signal unit to form the immunocomplex.	Low-field nuclear magnetic resonance	Zhang et al., 2024
3.		Pathogen is captured by capture unit on magnetic glassy carbon electrodes, recognized by detector unit	Electrochemiluminescence and anodic stripping voltammetry	Wang et al., 2019
4.		Detection of pathogen, by employing giant Au vesicles with anchored tiny gold nanowires (AuNW) as a smart probe.	Colorimetric and surface-enhanced Raman scattering (SERS)	Guo et al., 2018
5.	<i>V. vulnificus</i>	Piezoelectric wafer attached with two gold electrodes used as the transducer and immobilized antibody on the sensor chip.	Piezoelectric	Hong et al., 2014

6.	<i>V. alginolyticus</i>	Synthesis of multi-walled carbon nanotubes (MWCNTs), which functioned as immuno-, magnetic, fluorescent sensors in detecting.	Fluorescence	Liu et al., 2014
BACTERIOPHAGE- BASED SENSORS				
7.	<i>V. cholerae</i>	Engineered phages allowed the binding of gold nanoparticles, which aggregate on the phages, resulting in a visible color change due to alteration of surface plasmon resonance properties.	Colorimetric	Peng et al., 2019
8.	<i>V. parahaemolyticus</i>	A one-step label-free colorimetric strategy based on M13 bacteriophage-displayed nanobody (phage-Nb) derived from camelid heavy-chain antibodies specific to <i>Vibrio parahaemolyticus</i> .	Colorimetric	Wang et al., 2023
APTASENSORS				
9.	<i>V. alginolyticus</i>	The HCR scaffold serves as a carrier for the aptamer, enabling assembly into multi-Apt to enhance its binding affinity.	Hybridization Chain Reaction	Zhao et al., 2023
10.	<i>V. alginolyticus</i>	Couples the DNA nanostructure-modified magnetic beads with a solid-contact polycation-sensitive membrane electrode for the detection.	Potentiometric	Zhao et al., 2016

Immunosensors employing antigen-antibody interactions are reliable sensing methods, yet they face a significant drawback due to their costly development. Moreover, sensors based on bacteriophages exploit their ability to infect specific hosts but suffer from instability over extended periods and potential drying out of the phages. Hence, opting for aptamers as the bio-sensing component can offer practical advantages, being cost-effective, stable, and exhibiting specificity toward their targets.

2.4 Aptamers and Whole-cell SELEX

Aptamers are 25–80 bases long single-stranded functional DNA/RNA structures with high affinity and specificity for various targets such as small inorganic ions, bacteria, viruses, amino acids, organic molecules, proteins, whole cells, and animals (Zhou et al., 2017). Aptamers typically adopt a variety of three-dimensional structures that selectively bind to specific targets. Aptamers have several advantages, including ease of generation, low manufacturing cost, minimal batch-to-batch variability, reversible folding characteristics, and low immunogenicity compared to monoclonal antibodies (Zhang et al., 2019). Their most significant benefit lies in the ability to easily modify and engineer these oligonucleotide sequences into aptamer-drug conjugates and targeted delivery systems, enabling their clinical use in therapy (Zhou et al., 2017). Recently, numerous important applications have been demonstrated in therapeutic research.

In 1990, a selection process for aptamers called Systematic Evolution of Ligands by Exponential Enrichment (SELEX) was developed (Tuerk et al., 1990). Typically, a SELEX process begins with a chemically synthesized random RNA or single-stranded DNA (ssDNA) library containing 10^{13} to 10^{15} different sequence motifs. In the initial selection round, this library is

incubated directly with the target molecule. Oligonucleotides that bind to the target are eluted, amplified by PCR, and used in subsequent selection rounds. After several rounds of selection, high-affinity and target-specific oligonucleotides, known as aptamers, are obtained (Ylera et al., 2002).

Whole-cell SELEX is a modified method within SELEX technologies used to generate aptamers specifically bound to live bacteria (Medley et al., 2011). This process involves following steps: (a) screening random nucleic acids bound to the target bacteria, (b) repetitive separation and exponential amplification of the oligonucleotides, and (c) cloning and sequencing of the identified specific binding molecules (Torres-Chavolla et al., 2009). Aptamers obtained through whole-cell SELEX demonstrate high affinity and specificity for bacterial surface molecules and live bacterial targets (Moon et al., 2015). As whole-cell SELEX targets live pathogenic bacteria, aptamers can efficiently locate and bind to surface molecules on live bacteria compared to other SELEX approaches. Consequently, aptamers obtained through whole-cell SELEX may exhibit minimal cross-reactivity with non-target bacteria (Cao et al., 2009).

Aptamers are often compared to antibodies due to their target-recognition capability, selective binding, and affinity, in addition to unique features that offer more flexibility in development and application (Sefah et al., 2010). The generation of aptamers through the SELEX process is relatively quick. Additionally, aptamers are chemically synthesized, enabling the incorporation of various functional groups and specific moieties such as biotin, carboxyl, amino, and thiol, most of which do not interfere with target recognition (Hicke et al., 1996; Da Pieve et al., 2010). This flexibility allows for aptamer conjugation with drug molecules and nanoparticles.

Hence, aptamers are extensively employed as excellent molecular identifiers. The adoption of aptamer-based biosensors and bioassay techniques for bacterial detection is expected to replace

conventional methods, thereby enhancing the speed, sensitivity, specificity, and reliability of detection. However, the aptasensors designed for *Vibrio alginolyticus* diagnosis face challenges due to the intricate sample preparation and detection techniques involved. Hence, in this study we are designing biosensors with aptamers as the sensing element and a simple colorimetric detection using the visual color changing property of gold nanoparticles.

2.5 Optical biosensors

Optical biosensors function by detecting changes in optical signals resulting from the interaction between the analyte and bioreceptors. Due to their safety and high resolution, optical biosensors find extensive applications in detecting pathogenic bacteria when combined with aptamers (Damborský et al., 2016).

Aptamer-based colorimetric biosensors detect analytes through color changes by mechanisms, including enzyme-mediated substrate oxidation (Wu et al., 2015), catalyzed oxidation of nanomaterials (Hu et al., 2015), or the aggregation or disaggregation of nanoparticles (Mondal et al., 2018; Yousefi and Saraji, 2019). This approach bypasses the necessity for complex analytical instruments, therefore simplifying the aptamer-based colorimetric biosensor compared to many others. Table 2 provides a summary of aptasensors developed over various years for the detection of different pathogens in medical, food and water samples, employing the colorimetric detection method.

Table 2 Aptamer-based biosensors reported for different pathogen with colorimetric detection.

Sr. no.	Pathogen	Description	Applications	Detection Technique	References
1.	<i>Escherichia coli</i>	Lipopolysaccharides (LPS)-binding aptamer on the surface of nanoscale polydiacetylene (PDA) vesicle using peptide bonding between the carboxyl group of the vesicle and the amine group of the aptamer.	Clinical faecal specimens.	Optical/ Colorimetric	Wu et al., (2012)
2.	<i>Salmonella enteritidis</i>	Two high affinity aptamer showed alterations in color in proportion to the number of <i>S. enteritidis</i> cells	Clinical, environmental and food samples.		Zhang et al., (2019)
3.	<i>Aeromonas salmonicida</i>	Dual-model colorimetric and ratiometric fluorescent aptasensor based on the G-quadruplex-modified aptamer and g-C ₃ N ₄ for sensitive, reliable, and visual detection of the diseased bacteria in fishes.	Aquaculture, food safety,		Lu et al., (2023)
4.	<i>Salmonella typhimurium</i>	Novel composite of graphitic carbon nitride nanosheets and Cu ₂ O nanocrystals and interaction with aptamer.	Food and water quality		Tarokh et al.(2021)
5.	<i>Vibrio parahaemolyticus</i>	A simple visual colorimetric assay using magnetic nanoparticles (MNPs) and gold nanoparticles (AuNPs).	Food samples		Sadsri et al., (2020)

CHAPTER 3: MATERIALS AND METHODOLOGY

3.1 Materials

3.1.1 Chemicals used:

Tetra chloroauric acid ($\text{HAuCl}_4 \cdot 3\text{H}_2\text{O}$), Sodium citrate, Aptamers (Bioserve India), Manganese ferrite, Ammonia, Ascorbic acid, Phosphate buffer, Sodium chloride, Magnesium chloride, Potassium chloride, Tris-HCl, Binding buffer, N-(3-dimethylaminopropyl)-N'-ethylcarbodiimide hydrochloride (EDC), N-hydroxysuccinimide (NHS), Zobell marine broth and TCBS agar.

3.1.2 Apparatus

A 300 kV field emission gun-transmission electron microscope (TEM, FEI Tecnai G2, Oregon, United States), X-ray diffractometer (Rigaku SmartLab, Tokyo, Japan, Zeiss Scanning electron microscope (EVO 18 special edition, India), UV-Vis spectrophotometer (UV mini 1240 Shimadzu, Japan), Fourier transform infrared spectrometer (FTIR, Bruker alpha2), Micro table high speed refrigerated centrifuge (Centrifuge, Lab-i-Fuge LABINDIA, India), Incubator shaker (CIS-24 Plus REMI, India), and Hot mega power stirrer (HLS200, LABQUEST by Borosil, India) were used.

3.2 Synthesis of AuNPs

Gold nanoparticles can be easily conjugated with aptamers enabling the identification of specific signals. AuNPs were synthesized using the citrate reduction method (Storhoff et al., 1998). A solution of (1 mM) tetrachloroauric acid ($\text{HAuCl}_4 \cdot 3\text{H}_2\text{O}$) was boiled with vigorous stirring in a 250 mL flat-bottom flask equipped with a reflux condenser to maintain the reaction volume. Trisodium citrate (38.8 mM) was rapidly added to the solution, boiled for 15 minutes, resulting in a color change from pale yellow to dark red, indicating the formation of AuNPs.

The solution was boiled for 15 minutes and removed from the heat source. It was cooled to room temperature while stirring continued for an additional 20 minutes. The synthesized AuNPs were characterized using UV-vis spectrophotometer, Nano particle analyzer and transmission electron microscopy. The concentration of the AuNPs was calculated using Beer's law ($A = \epsilon cL$), using an extinction coefficient of $2.4 \times 10^8 \text{ Molar}^{-1} \text{ cm}^{-1}$ at 520 nm (Haiss et al., 2007). The AuNPs colloidal solution was diluted and then stored at 4 °C.

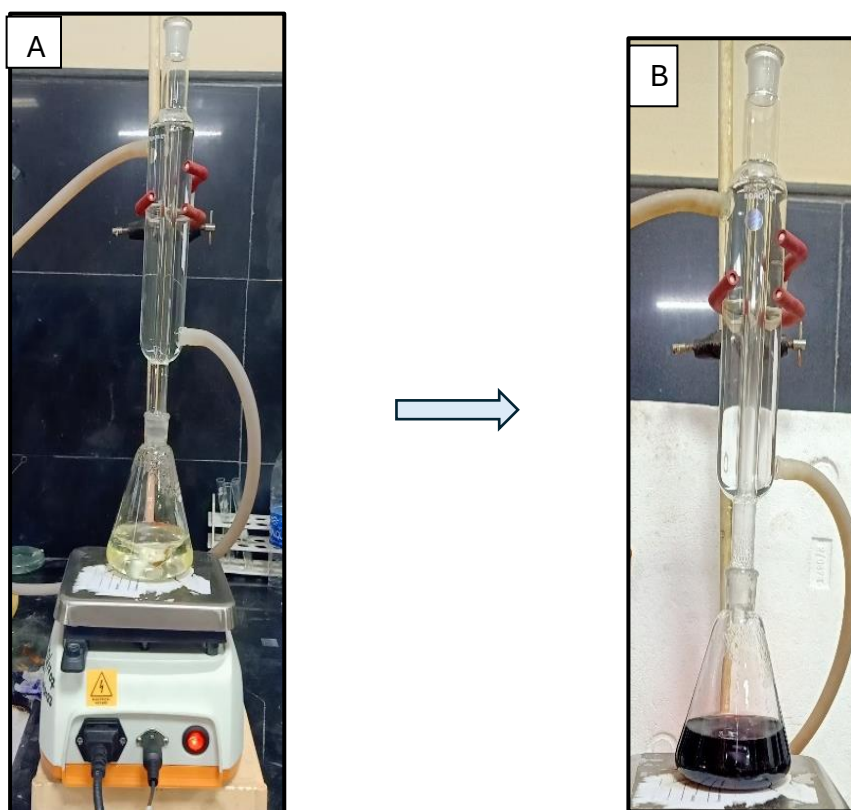


Figure 1 (A) Reflux condenser apparatus with gold solution (yellow) (B) Solution turns purple on adding trisodium citrate

3.3 Synthesis of carboxyl functionalized-MNPs

For isolation and enrichment of bacteria from other components in presence of external magnetic field MNPs are used. To synthesize MNPs (MnFe_2O_4), stoichiometric amount of $\text{MnCl}_2 \cdot \text{H}_2\text{O}$ and $\text{FeCl}_3 \cdot 6\text{H}_2\text{O}$ were weighed and dissolved in 70mL distilled water (Arsalani et al., 2018). The solution was stirred till a clear solution was obtained. Further concentrated ammonia solution was added dropwise till the pH of the solution was 10 with constant stirring. The solution was then transferred to the Teflon lined autoclave and kept in the oven at 180 °C for 24 hours. The solution was filtered and washed thrice with water followed by ethanol. It was dried at 80 °C in a hot air oven and the obtained powder was calcined at 500 °C for 3 hours in pre-heated muffle furnace.

For the carboxyl-functionalization of the MNPs, L-ascorbic acid and MnFe_2O_4 were taken in 1:2 ratio (Sorkhabi et al., 2020). AA was dissolved in 20mL double distilled water in a round bottom flask and MnFe_2O_4 solution was added dropwise. The mixture was stirred for 24 hours and then separated by centrifugation at 3000 rpm. It was washed thrice with double distilled water followed by ethanol and dried at 80 °C in a hot air oven. The magnetic property of MNPs was confirmed through observation of their attraction towards a magnet.

3.4 Identification and confirmation of aptamers

As per the findings reported in existing literature, the chosen aptamers have demonstrated notable specificity towards *Vibrio alginolyticus*, exhibiting minimal binding affinity towards other bacterial strains. These single-stranded DNA (ssDNA) aptamers were selected through Systematic Evolution of Ligands by Exponential enrichment (SELEX) methodology, specifically targeting the viable bacterial pathogen *V. alginolyticus*. The nucleic acid aptamer

designated for binding to AuNPs specific for *Vibrio alginolyticus* is represented by the following sequences: 5'SHGACGCTTACTCAGGTGTGACTCGCGTTTTATTGGTGTGGG GCTGGGGCGGTGGGTGGCTCTACTGGTTCCGTTCTGAAGGACGCAGATGAAGTCTC -3' (Yu et al., 2019). Additionally, nucleic acid aptamer for binding to MNPs is as follows: 5'-NH₂C₆ TCAGTCGCTTCGCCGTCTCCTTCAGCCGGGGTGGTCAGTAGGAGCAGCAC AAGAGGGAGCACAAGAGGGAGACCCAGAGGG-3' (Zheng et al., 2015). The oligonucleotides were supplied in a lyophilized form by BioServe Biotechnologies, India. They were resuspended at a stock concentration of 100 μ M by adding 95.92 μ L and 88.82 μ L of nuclease free water to the aptamers that were conjugated to MNPs and AuNPs respectively.

3.5 Preparation of Apt-AuNPs

The Apt-AuNPs conjugate were prepared based on a previously published method with slight modifications (Chen et al., 2012). This procedure involved a ligand exchange reaction between the thiol-functionalized aptamer (SH-aptamer) and the citrate-capped AuNPs, utilizing the well-known gold-sulfur chemistry. SH-aptamer (10 μ M) was added to the AuNP colloidal suspension (12 nM). After allowing the mixture to stand for 24 hours, the Apt-AuNP complex was aged by adding phosphate buffer to reach a final concentration of 10 mM. The suspension was left to stand for an additional 6 hours before 1 M NaCl. The suspension was further incubated for 34 hours at room temperature, followed by centrifugation for 30 minutes at 12,000 rpm to remove excess oligonucleotides. After discarding the supernatant, the red pellets were washed, recentrifuged, and resuspended in 1 mL of binding buffer.

3.6 Preparation of Apt-MNPs

The attachment of the aptamer to carboxyl functionalized MNPs to form the Apt-MNPs conjugate was accomplished through the formation of an amide bond (Ocsoy et al., 2021). Initially, the carboxyl groups present on the MNPs surface were activated using EDC/NHS mixture, allowing the amine groups on the aptamer oligonucleotides to be covalently bonded. Briefly, carboxyl functionalized MNP colloidal solution (10 mg/mL) was added with a fresh mixture of EDC (50 mg/mL) and NHS (50 mg/mL). This mixture was then incubated at room temperature gently mixing for 30 minutes, followed by magnetic separation to remove excess reagents. The resulting MNPs were then dispersed in 50 μ L of DI water, and NH_2 -aptamers (100 μ M) were added. This mixture was further incubated for 45 minutes at room temperature while continuous mixing. Subsequently, the Apt-MNPs were collected using a magnet, washed with deionized water, and suspended in 500 μ L of distilled water.



Figure 2 Optical image of Apt-MNPs

3.7 Characterization of NPs and Apt-NP conjugates

The AuNPs and MNPs were characterized using a combination of techniques to determine their size, shape, surface properties, stability, and optical properties. The UV-Vis spectrum of the AuNPs exhibited a prominent absorption peak at 522 nm, indicative of the size and concentration of AuNPs. TEM/SEM imaging, XRD patterns, FTIR spectra, and zeta potential analysis were used for the property analysis of the NPs (AuNPs and MNPs) and their aptamer conjugates (Song et al., 2008).

3.8 Standardization of bacterial concentration

V. alginolyticus was procured from MTCC, Chandigarh (MTCC 13127) in a lyophilized form. The ampoule was opened and the freeze-dried culture was suspended in ZMB, streaked on TCBS and Zobell marine agar and incubated at 30 °C for 24 hours as per the guidelines by MTCC. The culture was sub-cultured from the master stock, and both master and working stock were maintained. The growth curve of *V. alginolyticus* was studied to assess the colorimetric detection at different phases and concentrations. The bacteria were incubated for 24 hours at 30 °C in Zobell marine broth until it surpassed the logarithmic growth phase. Within subsequent intervals the sample was collected, and the optical density was measured at 600 nm. Plate counting methodology was employed to validate the bacterial count. The bacterial culture was diluted with 0.85 % saline and 100 µL of the culture was spread onto agar plates (TCBS agar), cultured at 30 °C for 24 hours to facilitate the enumeration of colony-forming units (CFU/mL). The results were used to calculate the minimum bacterial concentration required to carry out the optical-biosensor reaction.

3.9 Colorimetric detection

Based on the bacterial growth curve, a concentration of 5×10^3 CFU/mL was obtained during the exponential phase of growth at 12 hours. Therefore, for detecting *V. alginolyticus*, 150 μ L of synthesized Apt-AuNPs and 20 μ L of Apt-MNPs were added to the bacteria resuspended in binding buffer (5×10^3 CFU/mL obtained at 12 h). The mixture was then incubated for 10 minutes at room temperature with gentle shaking. Following incubation, magnetic separation was performed to isolate the nanoparticle-bound bacteria. The resulting sample was then ready for detection. A color change was observed in the solution, indicating binding of the aptamer-nanoparticle conjugate to the bacteria. Additionally, the absorbance of the supernatant was measured at 490 nm using an ELISA reader to confirm the color change.

3.10 Standardization of the minimum bacterial volume for the colorimetric detection

Subsequent to determining the concentration, the optimum volume of pathogen required to carry out the detection was optimized. Bacterial samples (1 mL) were centrifuged at 6,000 rpm for 15 minutes, resulting in the formation of a pellet, the supernatant was carefully discarded and resuspended in binding buffer (composed of 50 mM Tris-HCl at pH 7.4, 5 mM KCl, 100 mM NaCl, and 1 mM MgCl₂). Different volumes of the bacterial suspension (100 μ L, 200 μ L, 300 μ L and 400 μ L) were used to standardize the minimum bacterial sample volume required to indicate colorimetric detection (color change). The mixture was incubated for 10 minutes with gentle shaking and the optical density of the color change was measured at 490 nm with the help of ELISA reader.

3.11 Detection of *V. alginolyticus* in fish and shrimp's sample

Fresh fish and shrimp samples were procured from Taleigao market, Goa. For the detection of *Vibrio alginolyticus*, a smear of the fish gills and shrimp hepatopancreas was obtained using sterile cotton swabs in the laminar air flow chamber. The swabs were inoculated in 0.85% saline and serially diluted and plated on Thiosulfate-Citrate-Bile Salts-Sucrose (TCBS) agar and incubated at 30 °C for 18 hours. Following the incubation period, five distinct colonies were selected from the agar plates and subjected to the colorimetric assay (as mentioned in 3.11). The absorbance was measured at 490 nm wavelength to quantify the colorimetric response.



Figure 3 Raw fish and shrimp sample from local market

CHAPTER 4: RESULTS AND DISCUSSION

4.1 Synthesis and characterization of AuNPs

Colloidal gold nanoparticles (AuNPs), 100 mL were produced through the chemical reduction of tetrachloroauric acid (HAuCl_4) (34 mg). The appearance of a reddish solution (Fig.4) in the reaction mixture signifies the formation of AuNPs.



Figure 4 Red colloidal solution of AuNPs

4.1.1 UV spectral analysis: UV spectra of the AuNPs was recorded in the range of 400 – 800 nm, which showed a peak at 522 nm (Fig.5), indicating the presence of nanoparticles larger than 20 nm, approximately measuring between 15–30 nm in size (Borse et al., 2020).

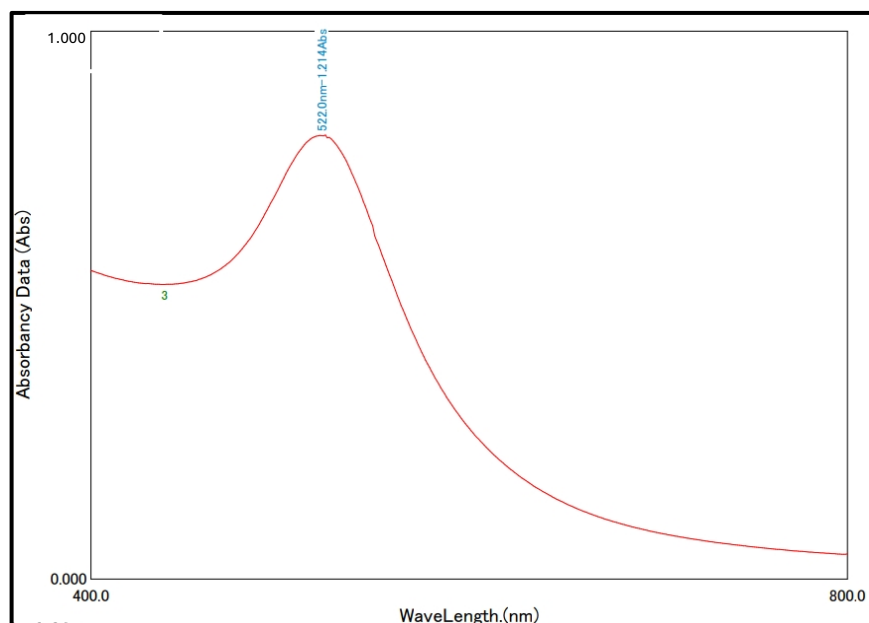


Figure 5 UV-Visible absorption spectra of AuNPs (Peak at 522 nm)

4.1.2 Electron microscopy: Scanning electron microscopy (SEM) was used to validate the synthesis of AuNPs and analyze the structure of the resulting AuNPs. The size and the particle shape distribution of the AuNPs was obtained by transmission electron microscopy (TEM). Fig 6 confirms the presence of AuNPs. The morphology of AuNPs revealed monodispersed spherical particles with a well-proportioned size (Fig 7). Their average diameter was 10-30 nm.

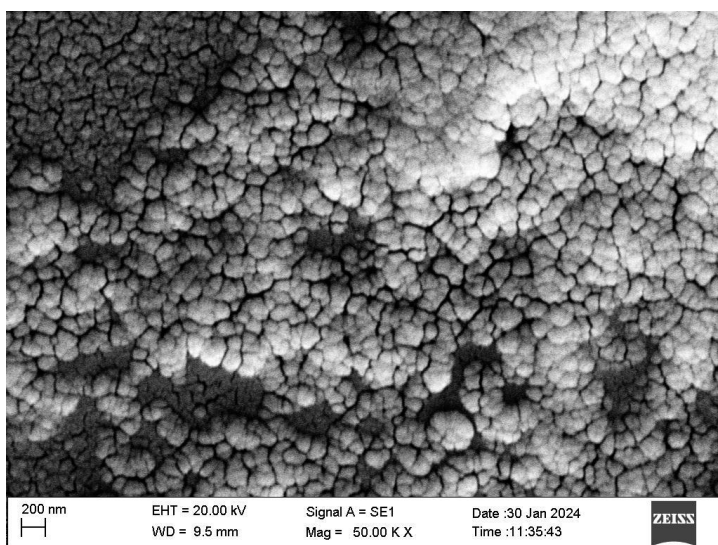


Figure 6 SEM image of AuNPs

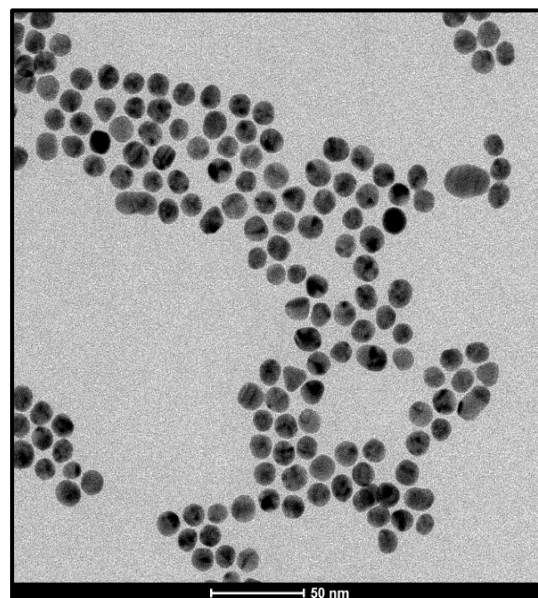


Figure 7 TEM image of AuNPs

4.1.3 Fourier Transform Infrared Spectroscopy analysis: FTIR spectra were analyzed using Origin 8 software (OriginLab Corporation, USA), version v8.0773(773) to identify the functional groups and chemical bonds present in the samples. Peak assignments were made based on established literature and spectral libraries. The spectra (Fig.8) reveal peaks at 3301 cm^{-1} and 1639 cm^{-1} suggesting the presence of functional groups on the surface of the nanoparticles. The peak at 3301 cm^{-1} corresponds to stretching vibrations of O-H bonds. The presence of hydroxyl group on the surface of gold nanoparticles can be attributed to the capping agents, confirming the presence of citrate groups used during synthesis. Peak at 1639 cm^{-1} is indicative of the presence of carbonyl groups (C=O stretching). It suggests the presence of stabilizing agents that contain carbonyl functional groups. The FTIR graph obtained shows similarity with the peaks suggested by Bhat et al., (2013).

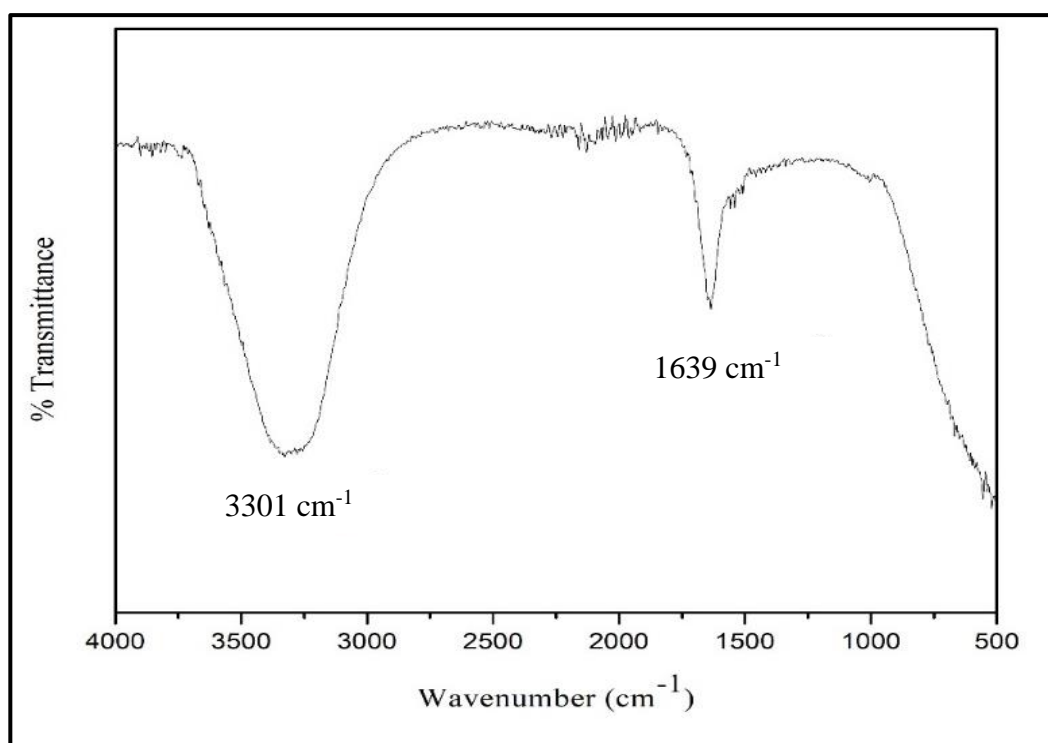


Figure 8 FTIR analysis of the AuNPs

4.1.4. Zeta potential: To study surface charge of the synthesized colloidal AuNPs, zeta potential measurements were carried out and it was observed to be -12.87 ± 0.907 mV (Fig.10). As suggested by (Borse et al., (2020)), the zeta potential of Au-NP is in the range of -10.6 to -37.7 mV, which is essential for the stability of AuNPs.

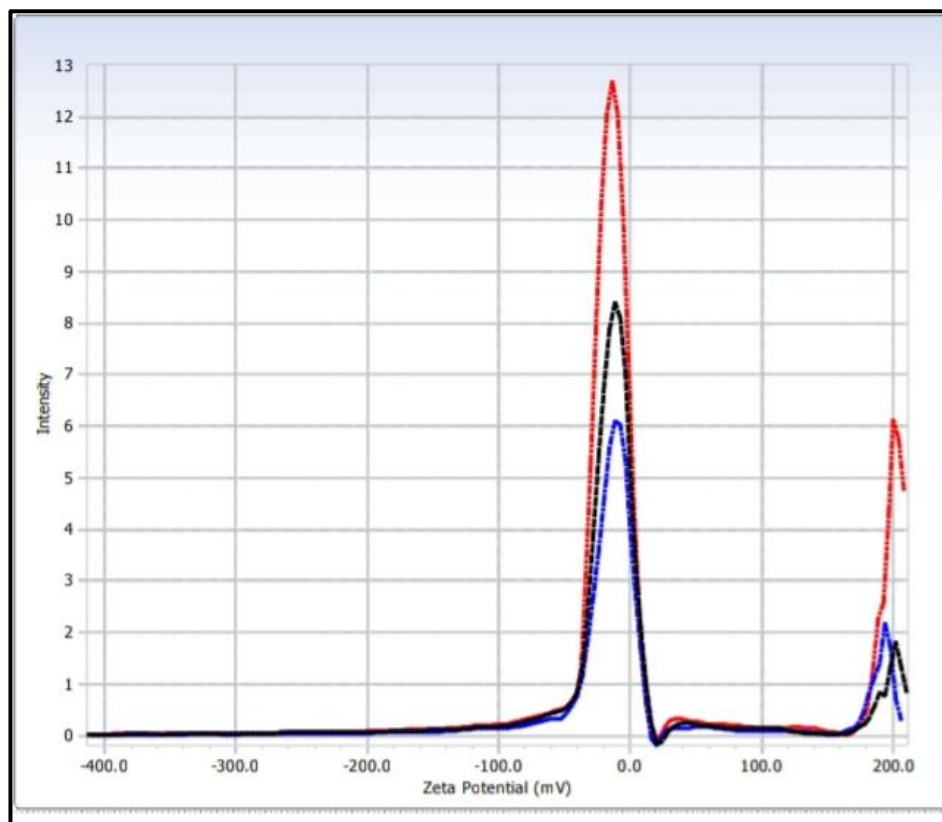


Figure 9 Zeta potential analysis of the AuNPs

4.2 Characteristics of Apt-AuNPs

4.2.1 UV-Vis spectral analysis: The attachment of thiol-aptamers to gold nanoparticles (AuNPs) via Au-S bonding was validated by the shift of the absorption peak from 522 to 526 nm (Fig.11). This is also confirmed by Sadsri et al., (2020) where an absorption peak shift of 524 to 528 nm was reported. This alteration in the surface charge of the Apt-AuNPs is likely attributed to the substitution of citrate molecules on the AuNP surface by thiol-aptamers. The conjugation of the aptamer imparted notable stability to the AuNPs, shielding them from aggregation in the presence of NaCl (Fig.12). Conversely, the unmodified AuNPs underwent aggregation upon exposure to NaCl, evidenced by a color change from red wine to violet (Fig.10).

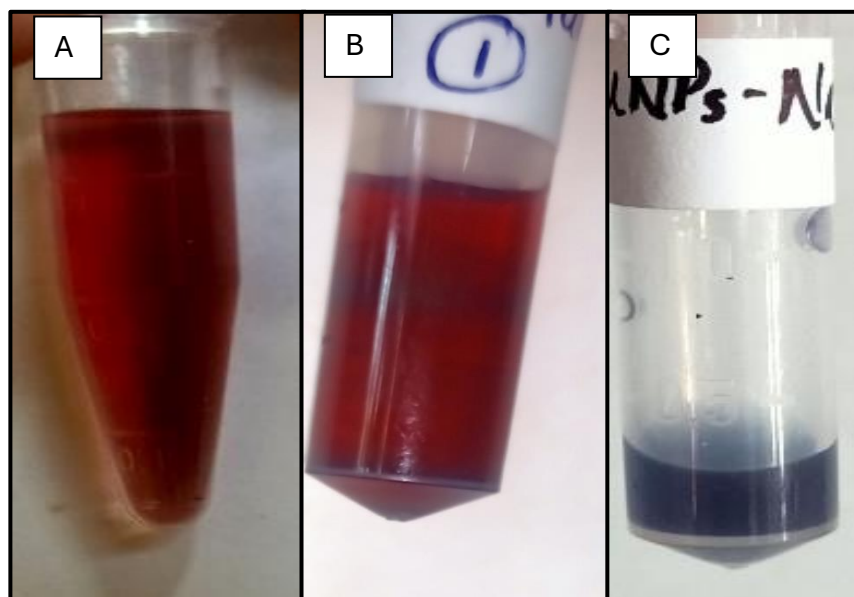


Figure 10 Optical images of (A)AuNPs, (B) Apt-AuNPs+ NaCl, (C) AuNPs+ NaCl respectively

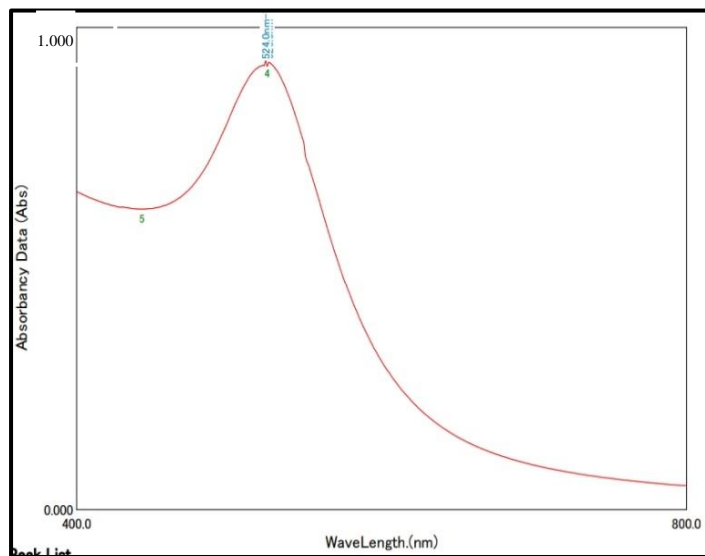


Figure 11 UV- Visible absorption spectra of Apt-AuNPs (Peak at 526 nm)

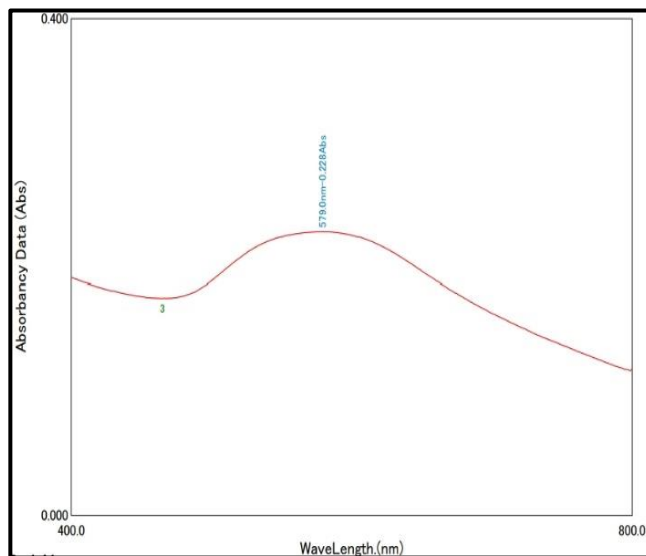


Figure 12 UV-Visible absorption spectra of AuNPs+ NaCl

4.2.2 FTIR analysis: The FTIR analysis for the Apt-AuNPs is depicted in Fig. 13. The appearance of peaks at 3309 cm^{-1} , 2112 cm^{-1} , and 1151 cm^{-1} indicates the presence of certain functional groups on the surface of the nanoparticles. At 3309 cm^{-1} the peak corresponds to the stretching vibrations of O-H bonds, similar to the peak observed in the previous analysis (Fig.8). The presence of this peak suggests the continued presence of hydroxyl groups, possibly from the aptamer molecules or the stabilizing agent. The 2112 cm^{-1} peak is indicative of the presence of $\text{C}\equiv\text{N}$ stretching vibrations, which are characteristic of nitrile functional groups.

In the context of the conjugation with aptamers, this peak likely arises from the aptamer molecules themselves, as they often contain nitrogen bases. The peak at 1151 cm^{-1} corresponds to the stretching vibrations of C-O bonds, suggesting the presence of organic ligands. These

ligands are often used to stabilize and functionalize the surface of nanoparticles, preventing their aggregation and providing sites for further functionalization.

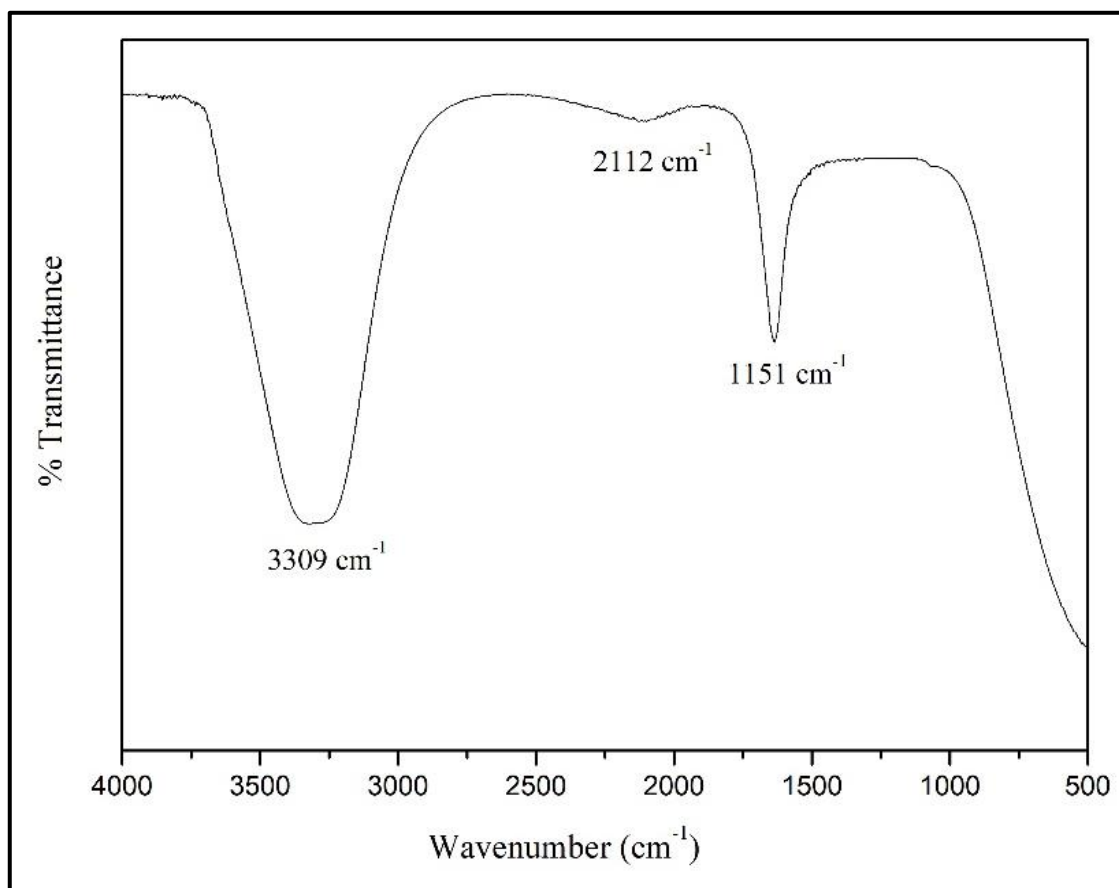


Figure 13 FTIR image of Apt-AuNPs conjugate

4.3 Synthesis and characterization of MNPs

MNPs were characterized for the confirmation of physical and chemical properties (size, structure, shape, crystallography and chemistry).

4.3.1: SEM analysis: The size and morphology of the MNP was assessed using scanning electron microscopy (SEM). Fig.15 demonstrates SEM images for the Fe_2O_4 MNPs having irregular shaped morphology with a particle size of 89 nm. As reported by Arsalani et al., (2017), MNP are characterized by a size range of 50-90 nm. The SEM image shows aggregated particles which could be due to SEM sample preparation process. The magnetic property was confirmed by magnetic test (Fig.14).

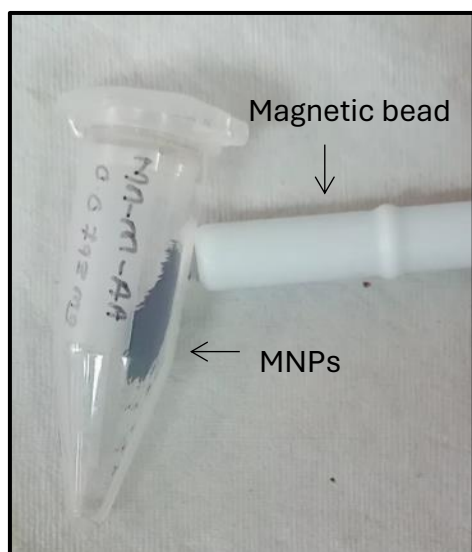


Figure 14 Test for magnetic property

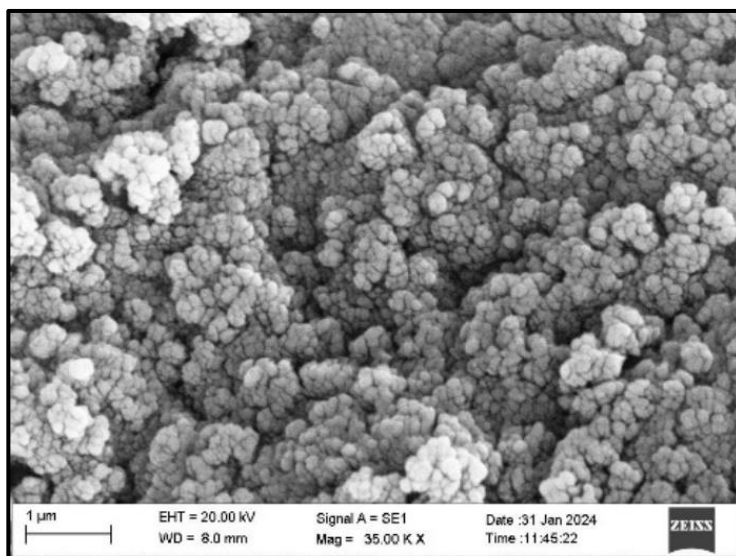


Figure 15 SEM image of MNPs

4.3.2: X-ray Diffraction: The profile of MnFe_2O_4 is shown below (Fig. 16). XRD analysis was carried out to characterize the phase formation and crystalline structure of the MnFe_2O_4 nanoparticles. The pattern confirms formation of pure Manganese ferrite by the peak position of 2θ values at 30.1° , 35.46° , 43.1° , 53.52° , 57.24° , 63° , 62.75° , 64.08° with standard JCPDS 75-0034. The results were on par with the characteristics of XRD of MNP suggested by (Arsalani et al., (2018), 29.6° , 35.1° , 42.6° , 56.4° and 62° . The average particle diameter can be estimated using Debye Scherer formula to be about 10 nm by using the strongest peak (311). All the diffraction peaks are significantly broadened, which indicates that the MnFe_2O_4 are polycrystalline in nature.

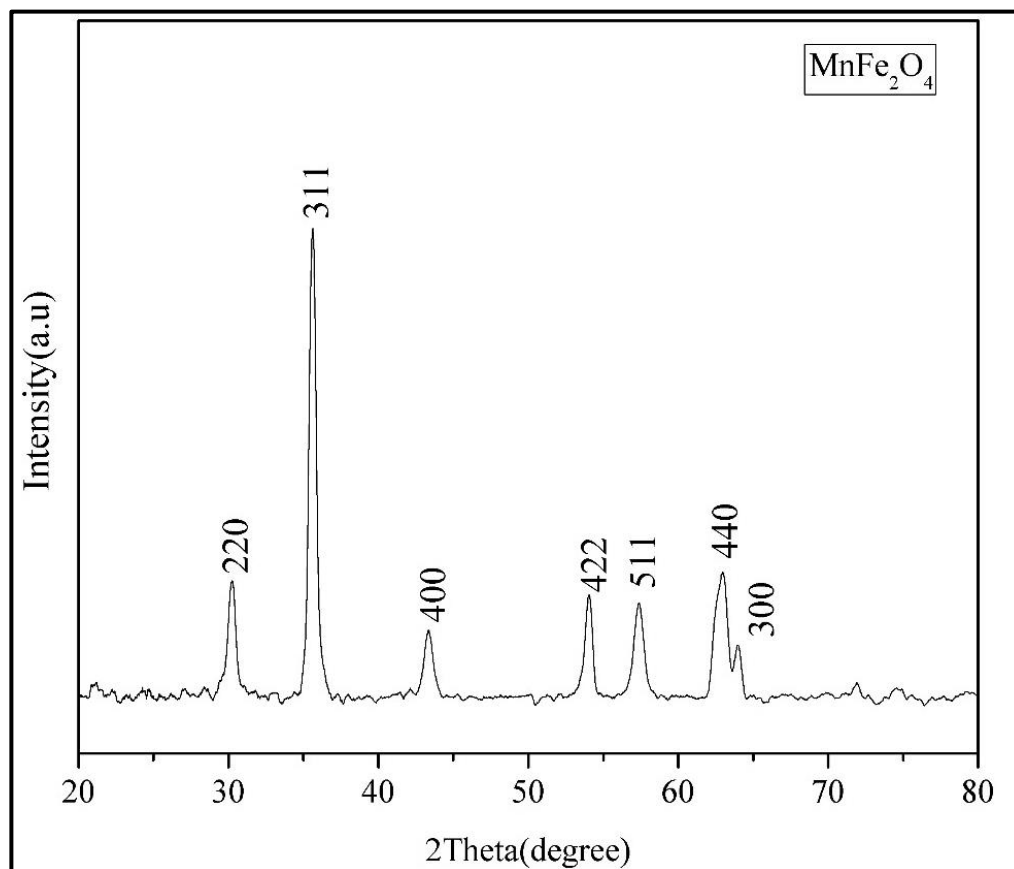


Figure 16 XRD pattern of MNPs

4.3.3: Fourier-Transform Infrared Spectroscopy: FTIR spectroscopy was used to confirm the functionalization of ascorbic acid on the MNPs. The characteristic peak of pure L-ascorbic acid is OH stretching at 3537 cm^{-1} , C=O stretching at 1754 cm^{-1} , C=C stretching at 1670 cm^{-1} and OH bending at 1321 cm^{-1} (Fig.17). The peak at 3537 cm^{-1} which can be seen in pure L-ascorbic acid is missing from the MNPs coated with ascorbic acid which indicates that the bonding to the MNPs has occurred through the OH group of the ascorbic acid (Fig.18). The other peaks which can be seen are C=C stretching at 1670 cm^{-1} , CH bending at 1215 cm^{-1} and M-O (metal oxygen) stretching at 686 cm^{-1} .

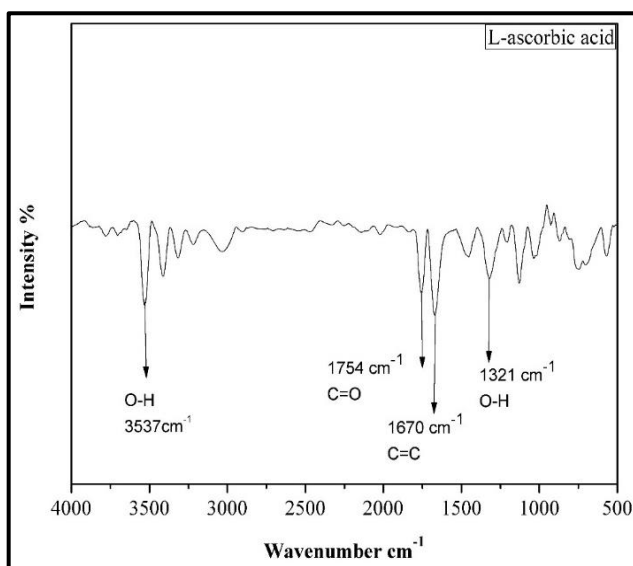


Figure 17 FTIR spectra of ascorbic acid

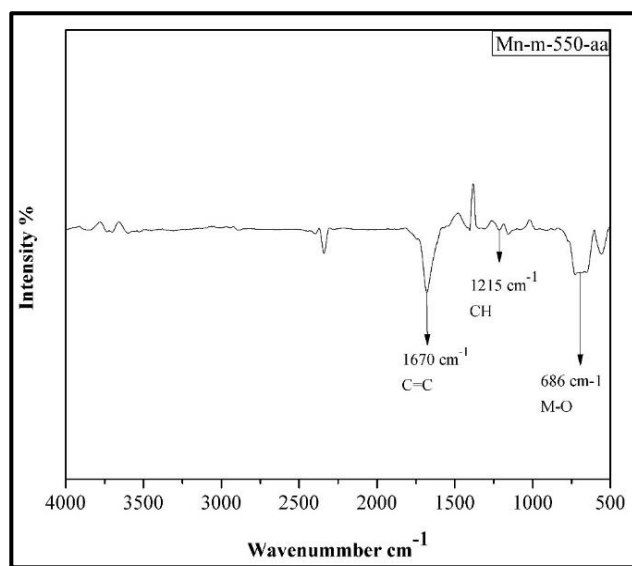


Figure 18 FTIR spectra of carboxyl functionalized MNPs

4.4 Characteristics of Apt-MNPs

4.4.1 Zeta potential: Following aptamer conjugation, the zeta potential value of carboxyl-functionalized magnetic nanoparticles (MNPs) decreased further from -3.58 ± 0.26 mV (Fig.19) to -1.97 ± 0.16 mV (Fig.20). This shift towards more negative values can be attributed to the inherent negative charge of DNA molecules. This result is in agreement with Sadsri et al., (2020).

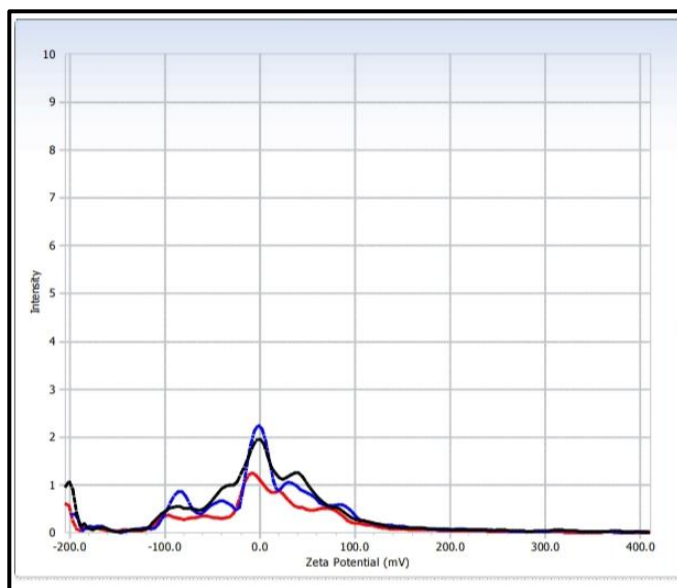


Figure 19 Zeta potential of MNPs

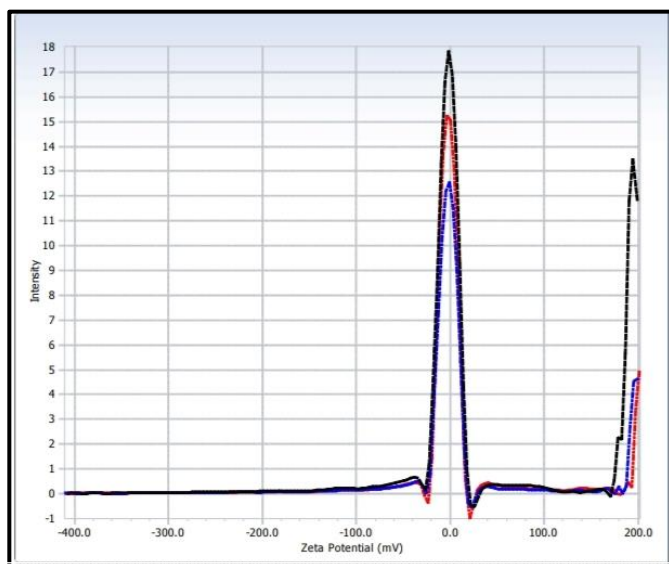


Figure 20 Zeta potential of Apt-MNPs

4.5 Standardization of bacterial concentration

The growth curve of *Vibrio alginolyticus* (Fig.21) was studied to optimize the conditions like concentration and to evaluate the apta-sensor accuracy at different growth phases of the pathogen. The concentration of *V. alginolyticus* on TCBS agar at 12 hours after incubation at 30 °C was calculated. The study revealed that it took 12 hours to reach exponential phase. The bacterial concentration (CFU/mL) was found to be 5×10^3 CFU/mL.

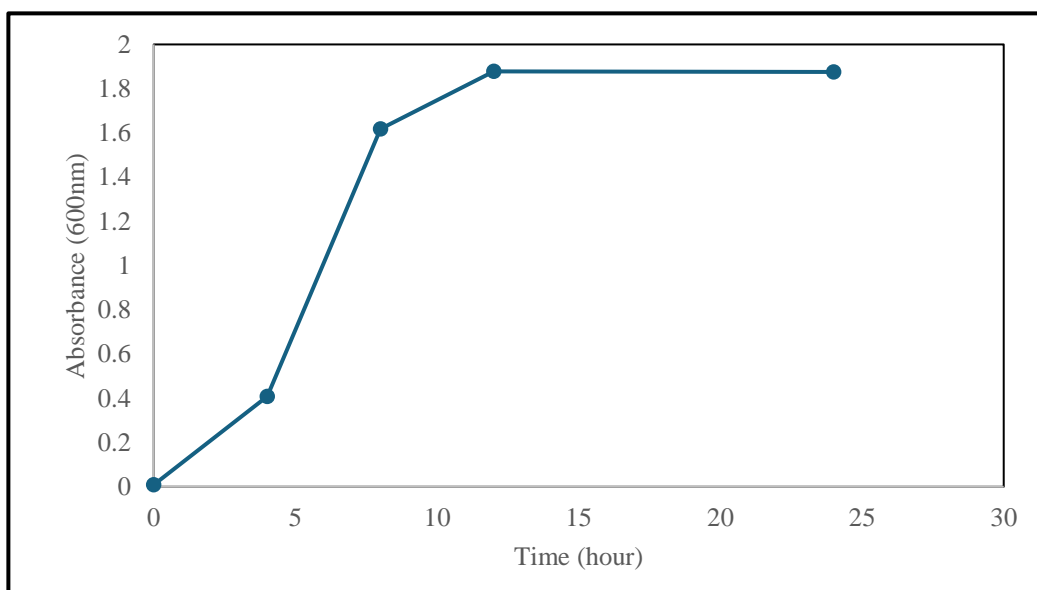


Figure 21 Growth curve of *V. alginolyticus*

The nanoparticles conjugate was mixed with different volume and concentration of pathogen to visualize color change. The change in absorbance at 490 nm is measured as the color changes from red to light pink (Sadsri et al., 2020). The results obtained from the experiment is given in table 3. As seen in the table, a decrease in the absorbance was seen at a bacterial concentration of 5×10^3 CFU/mL obtained at 4 hours of growth, indicating the presence of *V. alginolyticus*. This change in absorbance is attributed to the magnetic separation of bound bacteria by the

MNP-Apt conjugate, resulting in a clear solution and a visible color change from red to light pink thus lowering the absorbance. It was also observed that as the bacterial volume increase at 100 μL (5×10^2 CFU/mL), 200 μL (1×10^3 CFU/mL), 300 μL (1.5×10^3 CFU/mL) and 400 μL (2×10^3 CFU/mL), there was a decrease in absorbance seen.

Table 3 Optical density measured for different volumes of bacterial samples at different growth stages.

Bacterial sample	Optical Density at 490 nm of different volumes			
	100 μL	200 μL	300 μL	400 μL
Blank	0.204 ± 0.003	0.163 ± 0.002	0.132 ± 0.002	0.133 ± 0.01
4 hours	0.162 ± 0.006	0.034 ± 0.005	0.068 ± 0.003	0.003 ± 0.012
8 hours	0.218 ± 0.013	0.187 ± 0.002	0.176 ± 0.005	0.192 ± 0.002
12 hours	0.235 ± 0.010	0.324 ± 0.005	0.224 ± 0.007	0.234 ± 0.004
24 hours	0.466 ± 0.008	0.546 ± 0.004	0.695 ± 0.005	0.706 ± 0.008

As the concentration of the bacteria increased above 8 h, an increase in the absorbance values was observed. This indicated that the sandwich complex, involving the binding of magnetic nanoparticles, bacteria, and gold nanoparticles via specific aptamers, requires a higher volume of AuNP-Apt and MNP-Apt conjugate for a higher bacterial load. The results also indicate that the increased bacterial concentration might not be separating effectively from the solution during magnetic separation, leading to elevated absorbance readings. This could be rectified by increasing the MNP-Apt volume and also increasing the ascorbic acid (functionalization of the carboxyl group) coating on the MNPs, to efficiently separate the bacteria to obtain a clear

solution. Variations in particle size, shape, or magnetic strength could hinder their ability to bind effectively to the bacterial target and facilitate separation, contributing to the results.

The detection method used aptamers as a specific recognition tool, magnetic nanoparticles (MNPs) to capture the target, and gold nanoparticles (AuNPs) to detect signals. When the target bacteria were present, the aptamers on both MNPs and AuNPs attached to them, forming a "sandwich" structure. Apt-MNPs and Apt-AuNPs were incubated with *V. alginolyticus* cells and separated magnetically. As shown in Figure 22, the red color of the original AuNP suspension (Fig. 22A) faded significantly (Fig. 22B). This demonstrated that the "AuNP-aptamer-bacteria-Aptamer-MNP" conjugate designed in our study, formed a sandwich structure that could successfully provide a baseline report for the development of a nano-biosensor.

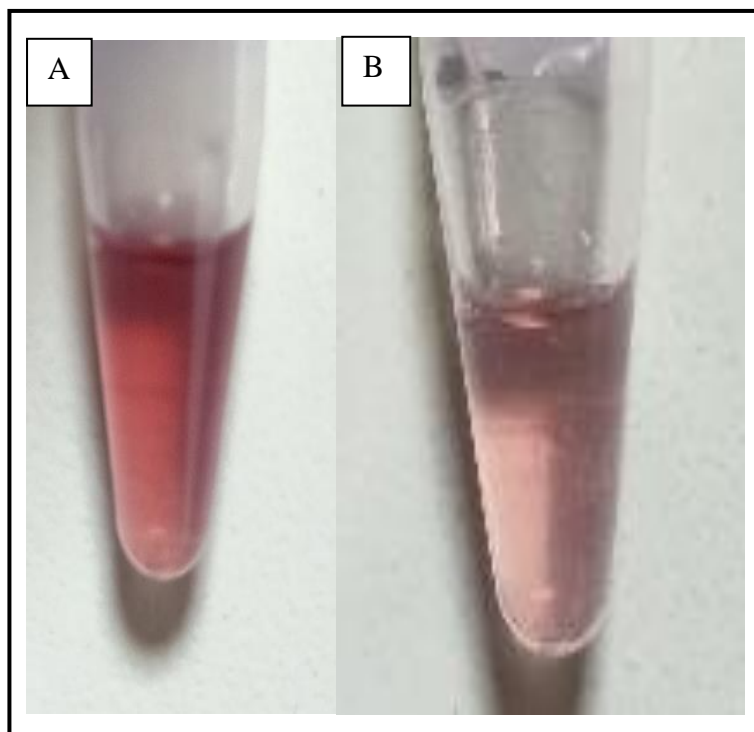


Figure 22 Optical images of the colorimetric detection (A) Apt-AuNPs+ MNPs+ buffer (B) Apt-AuNPs+ MNPs+ bacteria + buffer

4.6 Application of the developed conjugate for detection of *V. alginolyticus* in fish and shrimp sample

To confirm that this detection method works with unknown *V. alginolyticus* qualitatively raw shrimp and fish were bought from a local market to simulate the conditions. When plated on TCBS agar, three distinct colonies were observed from the shrimp hepatopancreatic region, while two distinct colonies were isolated from the fish gills (Fig.23). These isolates were used to test for specificity with the designed nanoparticle conjugates. As seen in Table 4 a decrease in the absorbance was seen when the nanoparticle-aptamer conjugates bound to shrimp colony 2 and 3. The results indicated the formation of a “sandwich” with these 2 colonies with respectively at a sample volume of 100 μ L. This confirms that the designed conjugate is suitable for detecting *V. alginolyticus* from a mixture of bacteria in real-time samples. However, this study requires further specificity tests to be carried out, by comparing it with negative controls (Eg. *Bacillus*, *E. coli* outgroups) and other *Vibrio* species, to confirm that there is no non-specific binding.



Figure 23 Isolated colonies from fish and shrimp sample on TCBS agar plates

Table 4 Absorbance of the samples at 490 nm

Sample	Absorbance (490 nm)
Blank (AuNP-Apt-MNP)	0.236 \pm 0.003
Shrimp swab	0.078 \pm 0.014
Shrimp colony 1	0.358 \pm 0.139
Shrimp colony 2	0.04 \pm 0.005
Shrimp colony 3	0.004 \pm 0.003
Fish colony 1	0.256 \pm 0.002
Fish colony 2	0.217 \pm 0.004

FUTURE PROSPECTS

1. To standardize the volume of Apt-MNPs and Apt-AuNPs conjugates in the reaction.
2. To check the specificity and non-specificity of the aptamers with other *Vibrio* species.
3. To standardize carboxyl functionalization of the MNPs.
4. Development of a strip based biosensor.

CONCLUSION

A simple yet efficient colorimetric assay for detecting *Vibrio alginolyticus*, utilizing magnetic nanoparticles (MNPs) and gold nanoparticles (AuNPs), has been successfully developed.

By incorporating aptamers as the bacterial-specific recognition element, this assay exhibits specificity and is more cost-effective compared to antibody-based systems. The magnetic separation of MNP-Apt-bacteria-Apt-AuNP complexes from the solution serves as an effective detection method, easily discernible by the naked eye due to a visible color change.

The designed sandwich structure would provide a baseline report for the development of a nano-biosensor strip. Moreover, this assay holds promise for broader applications, as it can be adapted for the detection of other foodborne pathogens or biological targets by simply substituting the biological recognition elements.

REFERENCE

1. Aguirre-Guzmán, G., H.M. Ruiz, and F. Asxencio. 2004. A review of extracellular virulence product of *Vibrio* species important in disease of cultivated shrimp. *Aquaculture Res* 35, 1395-1404.
2. Anderson J.W, and D.A. Conroy. 1970. *Vibrio* diseases in fishes. In: Snieszko SF (ed.): A Symposium on Diseases of Fishes and Shellfishes. Washington, D.C., American Fisheries Society, Special Publication No. 5, 266–272.
3. Arsalani, N., Tabrizi, A. G., & Ghadimi, L. S. (2018). Novel PANI/MnFe₂O₄ nanocomposite for low-cost supercapacitors with high-rate capability. *Journal of Materials Science: Materials in Electronics*, 29(7), 6077–6085.
4. Azarian, T., Ali, A., Johnson, J. A., Jubair, M., Cella, E., Ciccozzi, M., ... & Salemi, M. (2016). Non-toxigenic environmental *Vibrio cholerae* O1 strain from Haiti provides evidence of pre-pandemic cholera in Hispaniola. *Scientific reports*, 6(1), 36115.
5. Bargellini, A., Marchesi, I., Righi, E., Ferrari, A., Cencetti, S., Borella, P., & Rovesti, S. (2011). Parameters predictive of *Legionella* contamination in hot water systems: association with trace elements and heterotrophic plate counts. *Water research*, 45(6), 2315-2321.
6. Bhalla, N., Jolly, P., Formisano, N., & Estrela, P. (2016). Introduction to biosensors. June, 1–8.
7. Borse, V., & Konwar, A. N. (2020). Synthesis and characterization of gold nanoparticles as a sensing tool for the lateral flow immunoassay development. *Sensors International*, 1, 100051.
8. Buján, N., Toranzo, A. E., & Magariños, B. (2018). *Edwardsiella piscicida*: a significant bacterial pathogen of cultured fish. *Diseases of aquatic organisms*, 131(1), 59-71.
9. Buss, J. E., Cresse, M., Doyle, S., Buchan, B. W., Craft, D. W., & Young, S. (2019). *Campylobacter* culture fails to correctly detect *Campylobacter* in 30% of positive patient stool specimens compared to non-cultural methods. *European Journal of Clinical Microbiology & Infectious Diseases*, 38, 1087-1093.

10. Cai, S. H., Lu, Y. S., Wu, Z. H., & Jian, J. C. (2013). Cloning, expression of *Vibrio alginolyticus* outer membrane protein-Omp U gene and its potential application as vaccine in crimson snapper, *Lutjanus erythropterus* Bloch. *Journal of fish diseases*, 36(8), 695-702.
11. Cai, S.H., Wu, Z.H., Jian, J.C. and Lu, Y.S. (2007) Cloning and expression of gene encoding the thermostable direct hemolysin from *Vibrio alginolyticus* strain HY9901, the causative agent of vibriosis of crimson snapper (*Lutjanus erythropterus*). *J Appl Microbiol* 103, 289–298.
12. Cao, X., Li, S., Chen, L., Ding, H., Xu, H., Huang, Y., ... & Shao, N. (2009). Combining use of a panel of ssDNA aptamers in the detection of *Staphylococcus aureus*. *Nucleic acids research*, 37(14), 4621-4628.
13. Chauhan, A., Goyal, P., Varma, A., & Jindal, T. (2017). Microbiological evaluation of drinking water sold by roadside vendors of Delhi, India. *Applied Water Science*, 7, 1635-1644.
14. Chen, Q., Yan, Q., Wang, K., Zhuang, Z., & Wang, X. (2008). Portal of entry for pathogenic *Vibrio alginolyticus* into large yellow croaker *Pseudosciaena crocea*, and characteristics of bacterial adhesion to mucus. *Diseases of aquatic organisms*, 80(3), 181-188.
15. Chen, Z., Lei, Y., Chen, X., Wang, Z., & Liu, J. (2012). An aptamer-based resonance light scattering assay of prostate specific antigen. *Biosensors and Bioelectronics*, 36, 35–40.
16. Chong, R., Bousfield, B., & Brown, R. (2011). *Fish disease management. Veterinary Bulletin–Agriculture, Fisheries, and Conservation Department Newsletter (December 1):1(8):1–12.*
17. Chong, R., Bousfield, B., & Brown, R. (2011). *Fish Disease Management. Veterinary Bulletin - Agriculture, Fisheries and Conservation Department Newsletter, Hong Kong, December 1, 8.*
18. Da Pieve, C., Williams, P., Haddleton, D. M., Palmer, R. M., & Missailidis, S. (2010). Modification of thiol functionalized aptamers by conjugation of synthetic polymers. *Bioconjugate chemistry*, 21(1), 169-174.

19. Damborský, P., Švitel, J., & Katrlík, J. (2016). Optical biosensors. *Essays in biochemistry*, 60(1), 91-100.
20. De Jong, J. (2017). Aquaculture in India. Rijksdienst voor Ondernemen d Nederland.
21. Declercq, A. M., Haesebrouck, F., Van den Broeck, W., Bossier, P., & Decostere, A. (2013). Columnaris disease in fish: a review with emphasis on bacterium-host interactions. *Veterinary research*, 44(1), 1-17.
22. Duan, N., Wu, S., Dai, S., Gu, H., Hao, L., Ye, H., & Wang, Z. (2016). Advances in aptasensors for the detection of food contaminants. *The Analyst*, 141(13), 3942–3961.
23. Duan, N., Xu, B., Wu, S., & Wang, Z. (2016). Magnetic Nanoparticles-based Aptasensor Using Gold Nanoparticles as Colorimetric Probes for the Detection of *Salmonella typhimurium*. *Analytical sciences: the international journal of the Japan Society for Analytical Chemistry*, 32(4), 431–436.
24. Edwards, P., Zhang, W., Belton, B., & Little, D. C. (2019). Misunderstandings, myths and mantras in aquaculture: Its contribution to world food supplies has been systematically over reported. *Marine Policy*, 106, 103547.
25. El -Galil, M.A., and Mohamed, M.H. 2012. First Isolation of *Vibrio alginolyticus* from Ornamental Bird Wrasse Fish (*Gomphosus caeruleus*) of the Red Sea in Egypt. *Journal of Fisheries and Aquatic Science* 7:461 -467.
26. FAO. 2014 National Aquaculture Sector Overview India, p. 1; Ministry of Agriculture, Department of Animal Husbandry, Dairying and Fisheries. 2014. Handbook on Fisheries Statistics 2014, p. 5.
27. FAO. Fisheries and Aquaculture Software. FishStatJ: Software for Fishery and Aquaculture Statistical Time Series (FAO Fisheries Division, 2019).
28. Gill, A. (2017). The importance of bacterial culture to food microbiology in the age of genomics. *Frontiers in microbiology*, 8, 256356.
29. Guo, Z., Jia, Y., Song, X., Lu, J., Lu, X., Liu, B., Han, J., Huang, Y., Zhang, J., & Chen, T. (2018). Giant Gold Nanowire Vesicle-Based Colorimetric and SERS Dual-Mode Immunosensor for Ultrasensitive Detection of *Vibrio parahaemolyticus*. *Analytical chemistry*, 90(10), 6124–6130.

30. Haiss, W., Thanh, N. T., Aveyard, J., & Fernig, D. G. (2007). Determination of size and concentration of gold nanoparticles from UV–Vis spectra. *Analytical chemistry*, 79(11), 4215-4221.
31. Haldar, S., Maharajan, A., Chatterjee, S., Hunter, S. A., Chowdhury, N., Hinenoya, A., ... & Yamasaki, S. (2010). Identification of *Vibrio harveyi* as a causative bacterium for a tail rot disease of sea bream *Sparus aurata* from research hatchery in Malta. *Microbiological research*, 165(8), 639-648.
32. Hayrapetyan, H., Tran, T., Tellez-Corrales, E., & Madiraju, C. (2023). Enzyme-linked immunosorbent assay: types and applications. *ELISA: Methods and Protocols*, 1-17.
33. Hicke, B. J., Watson, S. R., Koenig, A., Lynott, C. K., Bargatze, R. F., Chang, Y. F., ... & Parma, D. (1996). DNA aptamers block L-selectin function in vivo. Inhibition of human lymphocyte trafficking in SCID mice. *The Journal of clinical investigation*, 98(12), 2688-2692.
34. Hinić, V., Amrein, I., Stammler, S., Heckendorn, J., Meinel, D., Frei, R., & Egli, A. (2017). Comparison of two rapid biochemical tests and four chromogenic selective media for detection of carbapenemase-producing Gram-negative bacteria. *Journal of microbiological methods*, 135, 66-68.
35. Hong, S., & Jeong, H. D. (2014). Development of piezoelectric immunosensor for the rapid detection of marine derived pathogenic bacteria, *Vibrio vulnificus*. *Journal of fish pathology*, 27(2), 99-105.
36. Hui-Min, L. I. U., Ju-Min, H. A. O., Jing, X. U., Qing-Pi, Y. A. N., Han, G. A. O., & Zheng, J. (2020). Selection and identification of common aptamers against both *Vibrio harveyi* and *Vibrio alginolyticus*. *Chinese Journal of Analytical Chemistry*, 48(5), 623-631.
37. Hushiarian, R., Yusof, N. A., Hushiarian, N., Abdullah, A. H., & Ahmad, S. A. A. (2015). Computer modeling to optimize the sensitivity of an optical DNA nanosensor. *Sensors and Actuators B: Chemical*, 207, 716-723.
38. Ibekwe, A. M., & Grieve, C. M. (2003). Detection and quantification of *Escherichia coli* O157: H7 in environmental samples by real-time PCR. *Journal of applied microbiology*, 94(3), 421-431.

39. Jansen, P.A., Kristoffersen, A.B., Viljugrein, H., Jimenez, D., Aldrin, M. & Stien, A. (2012) Sea lice as a density-dependent constraint to salmonid farming. *Proceedings of the Royal Society B: Biological Sciences*, 279, 2330–2338.
40. Jena, A. K., Biswas, P., & Saha, H. (2017). Advanced farming systems in aquaculture: strategies to enhance production. *Innovative Farming*, 1(1), 84-89.
41. Ji, Q., Wang, S., Ma, J., & Liu, Q. (2020). A review: progress in the development of fish *Vibrio* spp. vaccines. *Immunology Letters*, 226, 46-54.
42. Jørgensen, L. V. G. (2020). Zebrafish as a model for fish diseases in aquaculture. *Pathogens*, 9(8), 609.
43. Kahla-Nakbi, A. B., Besbes, A., Bakhrouf, A., & Alcaide, E. (2007). Characterisation and virulence properties of *Vibrio* isolates from diseased gilthead sea bream (*Sparus aurata*) cultured in Tunisia. *BULLETIN-EUROPEAN ASSOCIATION OF FISH PATHOLOGISTS*, 27(3), 90.
44. Kumar, A., Sarkar, T., & Solanki, P. R. (2023). Amine Functionalized Gadolinium Oxide Nanoparticles-Based Electrochemical Immunosensor for Cholera. *Biosensors*, 13(2), 177.
45. Lee, S., Khoo, V. S. L., Medriano, C. A. D., Lee, T., Park, S. Y., & Bae, S. (2019). Rapid and in-situ detection of fecal indicator bacteria in water using simple DNA extraction and portable loop-mediated isothermal amplification (LAMP) PCR methods. *Water research*, 160, 371-379.
46. Li, D., Liu, L., Huang, Q., Tong, T., Zhou, Y., Li, Z., Bai, Q., Liang, H., & Chen, L. (2021). Recent advances on aptamer-based biosensors for detection of pathogenic bacteria. *World journal of microbiology & biotechnology*, 37(3), 45.
47. Liao, I.C. and Leñaño, E.M. (Eds.). 2008. The aquaculture of groupers. Asian Fisheries Society.
48. Liu, C. H., Cheng, W., Hsu, J. P., & Chen, J. C. (2004). *Vibrio alginolyticus* infection in the white shrimp *Litopenaeus vannamei* confirmed by polymerase chain reaction and 16S rDNA sequencing. *Diseases of aquatic organisms*, 61(1-2), 169–174.
49. Liu, Y., Hu, J., Sun, J., Li, Y., Xue, S., Chen, X., Li, X., & Du, G. (2014, October 1). Facile synthesis of multifunctional multi-walled carbon nanotube for pathogen *Vibrio alginolyticus* detection in fishery and environmental samples. *Talanta*.

50. Loo, K.-Y., Law, J. W.-F., Tan, L. T.-H., Pusparajah, P., Letchumanan, V., & Lee, L.-H. (2022). Diagnostic techniques for rapid detection of *Vibrio* species. *Aquaculture*, *561*, 738628.
51. Luo, X., Fu, X., Liao, G., Chang, O., Huang, Z., & Li, N. (2017). Isolation, pathogenicity and characterization of a novel bacterial pathogen *Streptococcus uberis* from diseased mandarin fish *Siniperca chuatsi*. *Microbial Pathogenesis*, *107*, 380-389.
52. Maguire, M., Kase, J. A., Roberson, D., Muruvanda, T., Brown, E. W., Allard, M., ... & González-Escalona, N. (2021). Precision long-read metagenomics sequencing for food safety by detection and assembly of Shiga toxin-producing *Escherichia coli* in irrigation water. *PloS one*, *16*(1), e0245172.
53. Maldonado-Miranda, J. J., Castillo-Pérez, L. J., Ponce-Hernández, A., & Carranza-Álvarez, C. (2022). Chapter 19 - Summary of economic losses due to bacterial pathogens in aquaculture industry. In G. H. Dar, R. A. Bhat, H. Qadri, K. M. Al-Ghamdy, & K. R. Hakeem (Eds.), *Bacterial Fish Diseases* (pp. 399-417). Academic Press.
54. Manchanayake, T., Salleh, A., Amal, M. N. A., Yasin, I. S. M., & Zamri-Saad, M. (2023). Pathology and pathogenesis of *Vibrio* infection in fish: A review. *Aquaculture Reports*, *28*, 101459.
55. McCallum, H., Harvell, D. & Dobson, A. (2003) Rates of spread of marine pathogens. *Ecology Letters*, *6*, 1062–1067.
56. Medley, C. D., Bamrungsap, S., Tan, W., & Smith, J. E. (2011). Aptamer-conjugated nanoparticles for cancer cell detection. *Analytical chemistry*, *83*(3), 727-734.
57. Mehrotra, P. (2016). Biosensors and their applications—A review. *Journal of oral biology and craniofacial research*, *6*(2), 153-159.
58. Mei, X., Zhai, X., Lei, C., Ye, X., Kang, Z., Wu, X., ... & Wang, H. (2019). Development and application of a visual loop-mediated isothermal amplification combined with lateral flow dipstick (LAMP-LFD) method for rapid detection of *Salmonella* strains in food samples. *Food Control*, *104*, 9-19.
59. Metian, M., Troell, M., Christensen, V., Steenbeek, J., & Pouil, S. (2020). Mapping diversity of species in global aquaculture. *Reviews in Aquaculture*, *12*(2), 1090-1100.

60. Mohd-Aris, A., Muhamad-Sofie, M. H. N., Zamri-Saad, M., Daud, H. M., & Ina-Salwany, M. Y. (2019). Live vaccines against bacterial fish diseases: A review. *Veterinary World*, *12*(11), 1806.
61. Moon, J., Kim, G., Park, S. B., Lim, J., & Mo, C. (2015). Comparison of whole-cell SELEX methods for the identification of *Staphylococcus aureus*-specific DNA aptamers. *Sensors (Basel, Switzerland)*, *15*(4), 8884–8897.
62. Nnachi, R. C., Sui, N., Ke, B., Luo, Z., Bhalla, N., He, D., & Yang, Z. (2022). Biosensors for rapid detection of bacterial pathogens in water, food and environment. *Environment international*, *166*, 107357.
63. Nor -Amalina, Z. Dzarifah, M. Z. Mohd - Termizi, Y. Amal, M. N. A., Zamri -Saad, M. and Ina -Salwany, M. Y. 2017. Phenotypic and genotypic characterization of *Vibrio* species isolates from *Epinephelus* species in Selangor, Malaysia. In: Proceedings of the International Conference on Advances in Fish Health, 4 -6 April 2017, UPM Serdang, Malaysia.
64. Ocsoy, M. A., Yusufbeyoglu, S., Ildiz, N., Ulgen, A., & Ocsoy, I. (2021). DNA Aptamer-Conjugated Magnetic Graphene Oxide for Pathogenic Bacteria Aggregation: Selective and Enhanced Photothermal Therapy for Effective and Rapid Killing. *ACS Omega*, *6*(31), 20637-20643.
65. Peng, H., & Chen, I. A. (2019). Rapid Colorimetric Detection of Bacterial Species through the Capture of Gold Nanoparticles by Chimeric Phages. *ACS nano*, *13*(2), 1244–1252.
66. Pillay, T.V.R. & Kutty, M.N. (2005) *Aquaculture: Principles and Practices*, 2nd edn. Wiley-Blackwell, Oxford, UK.
67. Pires, N. M. M., Dong, T., Yang, Z., & da Silva, L. F. B. A. (2021). Recent methods and biosensors for foodborne pathogen detection in fish: progress and future prospects to sustainable aquaculture systems. *Critical reviews in food science and nutrition*, *61*(11), 1852–1876.
68. Poltronieri, P., Mezzolla, V., Primiceri, E., & Maruccio, G. (2014). Biosensors for the Detection of Food Pathogens. *Foods*, *3*, 511–526.

69. Rathore, G., Verma, D. K., Sharma, S. R., Sadhu, N., & Philipose, K. K. (2013). *Vibrio alginolyticus* infection in Asian seabass (*Lates calcarifer*, Bloch) reared in open sea floating cages in India.
70. Ringø, E. (2020). Probiotics in shellfish aquaculture. *Aquaculture and Fisheries*, 5(1), 1-27.
71. Rohani, M. F., Islam, S. M., Hossain, M. K., Ferdous, Z., Siddik, M. A., Nuruzzaman, M., ... & Shahjahan, M. (2022). Probiotics, prebiotics and synbiotics improved the functionality of aquafeed: Upgrading growth, reproduction, immunity and disease resistance in fish. *Fish & shellfish immunology*, 120, 569-589.
72. Sefah, K., Shangguan, D., Xiong, X., et al. (2010). Development of DNA aptamers using Cell-SELEX. *Nature Protocols*, 5, 1169–1185.
73. Selvin, J., & Lipton, A. P. (2003). *Vibrio alginolyticus* associated with white spot disease of *Penaeus monodon*. *Diseases of aquatic organisms*, 57(1-2), 147–150.
74. Song, S., Wang, L., Li, J., Fan, C., & Zhao, J. (2008). Aptamer-based biosensors. *TrAC Trends in Analytical Chemistry*, 27(2), 108-117.
75. Sorkhabi, S., Ghadermazi, M., & Mozafari, R. (2020). Adhesive functionalized ascorbic acid on CoFe₂O₄: a core-shell nanomagnetic heterostructure for the synthesis of aldoximes and amines. *RSC advances*, 10(68), 41336–41352.
76. Storhoff, J. J., Elghanian, R., Mucic, R. C., Mirkin, C. A., & Letsinger, R. L. (1998). One-pot colorimetric differentiation of polynucleotides with single base imperfections using gold nanoparticle probes. *Journal of the American Chemical Society*, 120(9), 1959-1964.
77. Su, Z., Li, Y., Pan, L., & Xue, F. (2016). An investigation on the immunoassays of an ammonia nitrogen-degrading bacterial strain in aquatic water. *Aquaculture*, 450, 17-22.
78. Tacon, A.G., 2020. Trends in global aquaculture and aquafeed production: 2000–2017. *Reviews in Fisheries Science & Aquaculture* 28(1), 43-56.
79. Thirumalaikumar, E., Lelin, C., Sathishkumar, R., Vimal, S., Anand, S. B., Babu, M. M., & Citarasu, T. (2021). Oral delivery of pVAX-OMP and pVAX-hly DNA vaccine using chitosan-tripolyphosphate (Cs-TPP) nanoparticles in Rohu, (Labeo

- rohita) for protection against *Aeromonas hydrophila* infection. *Fish & Shellfish Immunology*, *115*, 189-197.
80. Tian, F., Lyu, J., Shi, J., Tan, F., & Yang, M. (2016). A polymeric microfluidic device integrated with nanoporous alumina membranes for simultaneous detection of multiple foodborne pathogens. *Sensors and Actuators B: Chemical*, *225*, 312-318.
81. Torres-Chavolla, E., & Alocilja, E. C. (2009). Aptasensors for detection of microbial and viral pathogens. *Biosensors and bioelectronics*, *24*(11), 3175-3182.
82. Tuerk, C., & Gold, L. (1990). Systematic Evolution of Ligands by Exponential Enrichment: RNA Ligands to Bacteriophage T4 DNA Polymerase. *Science*, *249*, 505–510.
83. Wang, J., Ding, Q., Yang, Q., Fan, H., Yu, G., Liu, F., ... & Zhao, P. (2021). *Vibrio alginolyticus* triggers inflammatory response in mouse peritoneal macrophages via activation of NLRP3 inflammasome. *Frontiers in Cellular and Infection Microbiology*, *11*, 769777.
84. Wang, P., Yu, G., Wei, J., Liao, X., Zhang, Y., Ren, Y., Zhang, C., Wang, Y., Zhang, D., Wang, J., & Wang, Y. (2023). A single thiolated-phage displayed nanobody-based biosensor for label-free detection of foodborne pathogen. *Journal of hazardous materials*, *443*(Pt A), 130157.
85. Wang, T., Song, X., Lin, H., Hao, T., Hu, Y., Wang, S., Su, X., & Guo, Z. (2019). A Faraday cage-type immunosensor for dual-modal detection of *Vibrio parahaemolyticus* by electrochemiluminescence and anodic stripping voltammetry. *Analytica chimica acta*, *1062*, 124–130.
86. Yin, J. F., Wang, M. Y., Chen, Y. J., Yin, H. Q., Wang, Y., Lin, M. Q., ... & Hu, C. J. (2018). Direct detection of *Vibrio vulnificus*, *Vibrio parahaemolyticus*, and *Vibrio alginolyticus* from clinical and environmental samples by a multiplex touchdown polymerase chain reaction assay. *Surgical Infections*, *19*(1), 48-53.
87. Ylera, F., Lurz, R., Erdmann, V. A., & Fürste, J. P. (2002). Selection of RNA aptamers to the Alzheimer's disease amyloid peptide. *Biochemical and biophysical research communications*, *290*(5), 1583-1588.
88. Yoo, S. M., & Lee, S. Y. (2016). Optical Biosensors for the Detection of Pathogenic Microorganisms. *Trends in Biotechnology*, *34*, 7–25.

89. Zhai, L., Liu, H., Chen, Q., Lu, Z., Zhang, C., Lv, F., & Bie, X. (2019). Development of a real-time nucleic acid sequence-based amplification assay for the rapid detection of *Salmonella* spp. from food. *Brazilian Journal of Microbiology*, 50, 255-261.
90. Zhang, D., Chen, L., Lin, H., Hao, T., Wu, Y., Xie, J., Shi, X., Jiang, X., & Guo, Z. (2024). Well plate-based LF-NMR/colorimetric dual-mode homogeneous immunosensor for *Vibrio parahaemolyticus* detection. *Food chemistry*, 436, 137757.
91. Zhang, L., Huang, R., Liu, W., Liu, H., Zhou, X., & Xing, D. (2016). Rapid and visual detection of *Listeria monocytogenes* based on nanoparticle cluster catalyzed signal amplification. *Biosensors and Bioelectronics*, 86, 1-7.
92. Zhang, Y., Lai, B. S., & Juhas, M. (2019). Recent Advances in Aptamer Discovery and Applications. *Molecules*, 24(5), 941.
93. Zhao, G., Ding, J., Yu, H., Yin, T., & Qin, W. (2016). Potentiometric Aptasensing of *Vibrio alginolyticus* Based on DNA Nanostructure-Modified Magnetic Beads. *Sensors*, 16(12), 2052.
94. Zhao, Yifan & Luo, Sheng & Qiao, Zhaohui & Zhou, Qianjin & Fan, Jianzhong & Lu, Jianfei & Chen, Jiong. (2023). A Novel Method for Sensitive Detection of *Vibrio alginolyticus* Based on Aptamer and Hybridization Chain Reaction in Aquaculture. *Fishes*. 8. 477. 10.3390/fishes8100477.
95. Zhou, J., & Rossi, J. (2017). Aptamers as Targeted Therapeutics: Current Potential and Challenges. *Nature Reviews Drug Discovery*, 16(3), 181–202.